Towards sustainable heavy-duty transportation

Combustion and emissions using renewable fuels in a compression ignition engine

MAJA NOVAKOVIĆ
DEPARTMENT OF ENERGY SCIENCES | FACULTY OF ENGINEERING | LUND UNIVERSITY

Towards sustainable heavy-duty transportation

Towards sustainable heavy-duty transportation

Combustion and emissions using renewable fuels in a compression ignition engine

Maja Novaković

LUND
UNIVERSITY

Organization **LUND UNIVERSITY** Department of Energy Sciences	Document name **Doctoral Dissertation**	
Box 188 SE-221 00 Lund	Date of issue **2023-02-17**	
Author **Maja Novaković**	Sponsoring organization **KCFP Engine Research Center**	

Towards sustainable heavy-duty transportation: Combustion and emissions using renewable fuels in a compression ignition engine

Abstract

Transportation should become sustainable and available to everyone. Currently, transportation accounts for approx. one sixth of greenhouse gas (GHG) emissions globally, and heavy-duty trucks are responsible for almost 30% of that. When fossil diesel fuel is burned in a compression ignition engine, known as a diesel engine, it releases large amounts of CO_2, a GHG, into the air. GHGs confine heat in our atmosphere, causing global warming. Furthermore, the emissions are polluting air locally, having negative impact on human health and nature, but also some are adding to the global warming effects. Renewable diesel-like fuels, RME (rapeseed oil methyl ester) and HVO (hydrotreated vegetable oil), and light renewable or less carbon-intense alcohols, methanol and ethanol, as well as blended fuel E85 (ethanol and gasoline), can be used to reduce net CO_2 emissions, particulate matter (PM) and gaseous pollutants from the engine. They are available on the market and can be fed to diesel engines without major hardware modifications or by using the available technology. The aim of this PhD thesis was to investigate the effect of replacing fossil diesel fuel with renewable fuels, on the performance and local exhaust emissions of a heavy-duty diesel engine.

In experimental studies, particle size distributions in the exhaust were compared to those of fossil diesel. The origin of PM from these less-sooting fuels was studied. The compositions of organic aerosol (OA) and secondary organic aerosol (SOA) from HVO, RME and fossil diesel were analyzed, and the effect of a diesel oxidation catalyst (DOC) was evaluated. Formation of SOA in the atmosphere was simulated by aging emissions in an oxidation flow reactor. The nanostructure of the soot when operating on RME, diesel, methanol or ethanol was studied. Finally, the viability of using E85 fuel in a production truck engine was tested.

Ethanol and methanol proved to be nearly non-sooting fuels, with the nanoparticles in the exhaust originating primarily from the lubrication oil. The engine performed well with E85 fuel, with almost all raw emissions below the current legislated levels for one operation setting.

PM emissions were significantly lower when fossil diesel was replaced with HVO or RME. The chemical composition of OA was likely dominated by lubrication oil for all three diesel-like fuels. RME reduced both the OA emissions and changed the composition with evidence for minor fuel contributions in the mass spectra. The unregulated nanoparticles of size between 5 nm and 23 nm, which are also thought to originate from the lubrication oil, were emitted in high numbers as nucleation mode. RME and diesel branched soot agglomerates were composed of several tens to hundreds of primary particles, and diesel soot also contained fly ashes from burned engine lubrication oil. SOA formation was substantially lower for RME compared to fossil diesel and HVO. The DOC strongly reduced primary organic emissions in both the gas (hydrocarbons) and particle phase (OA), and only marginally affected OA composition. The DOC was also effective in reducing SOA formation upon atmospheric aging.

In order to defossilize transportation, all available technology and research efforts need to get united. When it comes to the heavy-duty sector, the most straightforward solution would be to replace fossil diesel fuel with a diesel-like fuel of non-fossil origin, beginning with the existing vehicle fleets. The use of HVO, RME and light alcohols would have a positive impact on an overall PM reduction.

Key words: **RME, HVO, E85, methanol, ethanol, decarbonization, defossilization, heavy-duty, compression ignition engine, low temperature combustion, PPC, emissions, PM, particles, aerosol, OA, SOA, DOC**	
Supplementary bibliographical information	Language: **English**
ISSN **0282-1990**	ISBN **978-91-8039-504-5** (print) **978-91-8039-505-2** (electronic)
Recipient's notes	Number of pages: **99**
	Security classification

Signature

Date 2023-01-13

Towards sustainable heavy-duty transportation

Combustion and emissions using renewable fuels in a compression ignition engine

Maja Novaković

LUND

UNIVERSITY

To my parents, Sanja & Dragoje,
for preparing me well for the exams of life

Table of Contents

Abstract

Transportation should become sustainable and available to everyone. Currently, transportation accounts for approx. one sixth of greenhouse gas (GHG) emissions globally, and heavy-duty trucks are responsible for almost 30% of that. When fossil diesel fuel is burned in a compression ignition engine, known as a diesel engine, it releases large amounts of CO_2, a GHG, into the air. GHGs confine heat in our atmosphere, causing global warming. Furthermore, the emissions are polluting air locally, having negative impact on human health and nature, but also some are adding to the global warming effects. Renewable diesel-like fuels, RME (rapeseed oil methyl ester) and HVO (hydrotreated vegetable oil), and light renewable or less carbon-intense alcohols, methanol and ethanol, as well as blended fuel E85 (ethanol and gasoline), can be used to reduce net CO_2 emissions, particulate matter (PM) and gaseous pollutants from the engine. They are available on the market and can be fed to diesel engines without major hardware modifications or by using the available technology. The aim of this PhD thesis was to investigate the effect of replacing fossil diesel fuel with renewable fuels, on the performance and local exhaust emissions of a heavy-duty diesel engine.

In experimental studies, particle size distributions in the exhaust were compared to those of fossil diesel. The origin of PM from these less-sooting fuels was studied. The compositions of organic aerosol (OA) and secondary organic aerosol (SOA) from HVO, RME and fossil diesel were analyzed, and the effect of a diesel oxidation catalyst (DOC) was evaluated. Formation of SOA in the atmosphere was simulated by aging emissions in an oxidation flow reactor. The nanostructure of the soot when operating on RME, diesel, methanol or ethanol was studied. Finally, the viability of using E85 fuel in a production truck engine was tested.

Ethanol and methanol proved to be nearly non-sooting fuels, with the nanoparticles in the exhaust originating primarily from the lubrication oil. The engine performed well with E85 fuel, with almost all raw emissions below the current legislated levels for one operation setting.

PM emissions were significantly lower when fossil diesel was replaced with HVO or RME. The chemical composition of OA was likely dominated by lubrication oil for all three diesel-like fuels. RME reduced both the OA emissions and changed the composition with evidence for minor fuel contributions in the mass spectra. The unregulated nanoparticles of size between 5 nm and 23 nm, which are also thought to originate from the lubrication oil, were emitted in high numbers as nucleation mode. RME and diesel branched soot agglomerates were composed of several tens to hundreds of primary particles, and diesel soot also contained fly ashes from burned engine lubrication oil. SOA formation was substantially lower for RME compared to fossil diesel and HVO. The DOC strongly reduced primary organic emissions in both the gas (hydrocarbons) and particle phase (OA), and only

marginally affected OA composition. The DOC was also effective in reducing SOA formation upon atmospheric aging.

In order to defossilize transportation, all available technology and research efforts need to get united. When it comes to the heavy-duty sector, the most straightforward solution would be to replace fossil diesel fuel with a diesel-like fuel of non-fossil origin, beginning with the existing vehicle fleets. The use of HVO, RME and light alcohols would have a positive impact on an overall PM reduction.

Popular scientific summary in Swedish

Populärvetenskaplig sammanfattning

Människor behöver ta sig från en punkt till en annan varje dag och varor måste nå sina destinationer. Transporter och leveranser som idag är dieseldrivna måste vara tillgängliga för alla och genomföras på ett för sig alla hållbart sätt. Vårt samhälle skulle klara oss väldigt kort tid om alla dieselmotorer helt plötsligt slutar fungera. Utmaningen samhället står inför är att minska antalet döds- och sjukdomsfall till följd av skadliga föroreningar i luften och minska transportsektorns klimatpåverkan. Idag står den globala transportsektorn för ca en sjättedel av utsläppen av växthusgaser. Tunga lastbilar står för cirka 5 procent av de globala växthusgasutsläppen.

En del av lösningen till detta problem skulle kunna vara förnybara bränslen som tillverkas genom hållbara biologiska eller kemiska processer från restprodukter inom avfalls- och matindustrin eller jord- och skogsbruk.

Den konventionella motorn med kompressionständning, även känd som en dieselmotor, dominerar lastbilsmarknaden på grund av dess låga bränsleförbrukning och höga vridmoment. Dieselmotorn har genomgått en teknisk revolution de senaste 20 åren och använder en högutvecklad teknik som också har en lovande framtid.

Nackdelen är att under förbränningen av fossil diesel i en dieselmotor släpps det ut stora mängder av växthusgasen koldioxid (CO_2) i luften. Växthusgaser gör att värmen behålls i atmosfären i stället för att stråla ut i rymden, vilket i sin tur orsakar global uppvärmning. Konsekvenserna för jorden och naturen kan vara enorma. Vi kan se en risk för snabbt smältande glaciärer, vattenbrist, fler bränder, naturkatastrofer och kustsamhällen som suddas ut p.g.a. stigande havsnivåer. Förutom koldioxid innehåller avgaserna andra föroreningar i gasfas, som kolmonoxid, kväveoxider, och organiska gaser, men även väldigt små dieselpartiklar som består av sot och organiska ämne. Avgasutsläppen förorenar luften lokalt, vilket har en stor negativ hälsopåverkan. Hos människor orsakar långvarig utsättning för dieselångor cancer, luftvägssjukdomar, hjärt- och kärlsjukdomar, men ökar även risken för olika kroniska sjukdomar, för tidig födsel, låg födelsevikt och antalet missfall.

Förnybara dieselliknande bränslen, RME (rapsmetylester) och HVO (vätebehandlad vegetabilisk olja), och förnybara eller mindre kolintensiva lätta alkoholer som metanol och etanol, samt förblandat bränsle E85 (etanol med lite bensin) kan användas för att minska nettoutsläppen av CO_2, liksom partiklar och gasformiga föroreningar från motorns avgaser. Dessa bränslen finns tillgängliga på tankstationer och kan användas i dieselmotorer med stöd av tillgängliga tekniska lösningar och utan några större hårdvaruändringar. Nya förbränningskoncept kan

också bidra till förbättring samt efterbehandlingssystem som tar bort hälsoskadliga ämnen i avgasröret.

Det övergripande syftet med denna doktorsavhandling var att undersöka effekten av att ersätta fossil dieselbränsle med förnybara dieselliknande bränslen och alkoholbränslen på en lastbilsmotors prestanda och avgaser. Arbetet omfattade både en litteraturstudie och fullskaliga experiment i en motorprovcell. Vi har jämfört mängd, storleksfördelningar, sammansättning och ursprung av partiklar i avgaserna från RME och HVO samt etanol och metanol med fossil diesel. Vi har också utvärderat effekten av dieseloxidationskatalysator (DOC) på organiska ämnen i partikelfas. Avslutningsvis har vi testat användbarhet av E85 bränsle i en produktionsvariant av en lastbilsdieselmotor och modellerat påverkan av parametrar som styr E85-förbränningsprocesser. Alla experiment utfördes vid en låg och mellan-till-låg motordriftsbelastning i en lastbilsmotor anpassad för användning i ett laboratorium. Dessa lägre laster motsvarar körförhållanden hos lastbilar som utför distribution, budtransporter och avfallshämtning i stadsmiljöer där vi egentligen vill minska utsläpp av skadliga föroreningar i luften.

Vi kan från våra och andra forskares studier dra slutsatser att mängden sotpartiklar minskas kraftigt genom att ersätta fossil diesel med etanol eller metanol. En avsevärd minskning syns även för HVO och RME. Vi kan bekräfta att de minsta partiklarna, nanopartiklarna, i avgaser inte kommer från bränsle utan från motorsmörjolja.

Motorn presterade bra med E85-bränsle och i ett driftläge understeg de flesta utsläpp de nuvarande lagstadgade nivåerna utan någon efterbehandling av avgaser. Bränslebytet minskade också utsläppen av kolväten och kolmonoxid från RME och HVO, vilket i sin tur minskade den sekundära aerosolbildningen och skulle därmed potentiellt sänka den totala atmosfäriska partikelmassan. Efterbehandlingssystemet bestående av DOC var mycket effektivt för att ta bort den organiska aerosolen i laboratoriestudierna för alla dieselliknande bränslen. Med förbättrad förståelse av utsläpp kan vi anpassa efterbehandlingssystem så att de släpper ut färre partiklar, och att de partiklar som eventuellt släpps ut är sådana som inte har dålig hälsopåverkan.

Det finns inte en enda lösning som kan minska koldioxidutsläpp från transportsektorn, men när det kommer till lastbilar så skulle den enklaste vägen vara att byta ut fossil diesel mot ett dieselliknande bränsle av icke-fossilt ursprung i den befintliga fordonsflottan. Resultaten i studierna visar tydliga miljö- och hälsovinster i att byta ut fossil diesel mot förnybara dieselliknande bränslen eller lätta alkoholer, även för en betydande del av dessa tunga fordon som fungerar utan system för borttagning av partiklar. Förnybara bränslen behövs inte bara för transport utan också som reservkraftverk. Kunskapen som presenteras i denna avhandling kan därför även tillämpas på hållbar elproduktion i avlägsna områden där det inte finns elnät.

List of publications

This thesis is based on the following publications:

Paper 1

Regulated Emissions and Detailed Particle Characterisation for Diesel and RME Biodiesel Fuel Combustion with Varying EGR in a Heavy-Duty Engine

Novakovic, M., Shamun, S., Malmborg, V. B., Kling, K. I., Kling, J., Vogel, U. B., Tunestal, P., Pagels, J. and Tuner, M.

SAE Technical Paper 2019-01-2291, **2019**, https://doi.org/10.4271/2019-01-2291

Paper 2

Detailed Characterization of Particulate Matter in Alcohol Exhaust Emissions

Shamun, S., **Novakovic, M.**, Malmborg, V. B., Preger, C., Shen, M., Messing M. E., Pagels, J., Tunér, M. and Tunestål, P.

COMODIA 2017 – 9th International Conference on Modeling and Diagnostics for Advanced Engine Systems, **2017**, https://doi.org/10.1299/jmsesdm.2017.9.B304

Paper 3

Detailed Analysis of Exhaust Emissions from Sustainable Diesel Like Fuels HVO and RME with Focus on Fresh and Aged Organic Aerosols

Novakovic, M., Eriksson, A., Gren, L., Malmborg, V. B., Shamun, S., Karjalainen, P., Svenningsson, B., Tuner, M., Verhelst, S., Pagels, J.

Manuscript submitted for publication and presentation at the SAE World Congress Experience WCX 2023, April 18-20, 2023 in Detroit, USA. Under review.

Paper 4

An Experimental Investigation of Directly Injected E85 Fuel in a Heavy-Duty Compression Ignition Engine

Novakovic, M., Tuner, M., Garcia, A. and Verhelst, S.

SAE Technical Paper 2022-01-1050, **2022**, https://doi.org/10.4271/2022-01-1050

The papers are re-printed with permission from the respective publishers.

Author's contributions to the included publications

Paper 1

I participated in the planning of the experiment. I operated the engine in the experiments. I made the major contribution in interpreting the data and making the conclusions. Also, I made the main contribution to the writing of the manuscript and led the peer-review process.

Paper 2

I shared the responsibility of carrying out the experiments and operating the engine with the first author. I contributed to the interpretation of the results, making conclusions and their presentation in the article. I contributed to the overall writing.

Paper 3

I contributed to the experimental planning. I participated in the experiments and ran the engine. I analyzed the engine data and interpreted the results. I made the major contribution in writing the manuscript, including selecting the scope of the paper. I have the main responsibility for the peer-review process.

Paper 4

I did the experimental planning and conducted the experiments. I analyzed the data, interpreted the results and formulated the conclusions. I wrote the manuscript and handled the peer-review process.

Peer-reviewed publications not included in this thesis

Characteristics of BrC and BC emissions from controlled diffusion flame and diesel engine combustion

Malmborg, V., Eriksson, A., Gren, L., Török, S., Shamun, S., **Novakovic, M.**, Zhang, Y., Kook, S., Tunér, M., Bengtsson, P.-E. and Pagels, J.

Aerosol Science and Technology, 55(7), 769-784, **2021**,
https://doi.org/10.1080/02786826.2021.1896674

Effects of renewable fuel and exhaust aftertreatment on primary and secondary emissions from a modern heavy-duty diesel engine

Gren, L., Malmborg, V. B., Falk, J., Markkula, L., **Novakovic, M.**, Shamun, S., Eriksson, A., Kristensen, T. B., Svenningsson, B., Tunér, M., Karjalainen, P. and Pagels, J.

Journal of Aerosol Science, 156, **2021**,
https://doi.org/10.1016/j.jaerosci.2021.105781

Particle emissions from a modern heavy-duty diesel engine as ice nuclei in immersion freezing mode: a laboratory study on fossil and renewable fuels

Korhonen K., Kristensen, T. B., Falk, J., Malmborg, V. B., Eriksson, A., Gren, L., **Novakovic, M.**, Shamun, S., Karjalainen, P., Markkula, L., Pagels, J., Svenningsson, B., Tunér, M., Komppula, M., Laaksonen, A., and Virtanen, A.

Atmospheric Chemistry and Physics, 22(3), 1615-1631, **2022**,
https://doi.org/10.5194/acp-22-1615-2022

Nomenclature

1G	first-generation
2G	second-generation
3G	third-generation
4G	fourth-generation
$\left(\dfrac{A}{F}\right)_S$	stoichiometric air-fuel ratio for the given fuel
AMS	aerosol mass spectrometry
ATDC	after top dead center
B20	a mixture of 20 volume-% RME and 80 volume-% fossil diesel
BBD	Box-Behnken design
BC	black carbon
BDC	bottom dead center
BEV	battery electric vehicle
Ca	calcium
CA5	start of combustion (SOC), the crank angle at which 5% of the charge has been consumed
CA50	the crank angle at which 50% of the charge has been consumed
CAD	crank angle degrees
CCN	cloud condensation nuclei
CDC	conventional diesel combustion
CH_4	methane
CHP	co-generation of heat and power
CLD	chemiluminescence detector
CO	carbon monoxide
CO_2	carbon dioxide
Cu	copper
DICI	direct injection compression ignition
DMS	differential mobility spectrometer
DOC	diesel oxidation catalyst
DOE	design of experiment

DPF	diesel particulate filter
EATS	exhaust aftertreatment system
eBC	equivalent black carbon
EDX	energy dispersive x-ray analysis
EGR	exhaust gas recirculation
EO	engine-out
EOI	end of injection
ERS	electric road system
Fe	iron
FFV	flexible-fuel vehicle
FID	flame ionization detector
FTIR	Fourier-transform infrared spectroscopy
GHG	greenhouse gas
GIE	gross indicated efficiency
HC	hydrocarbon
HCHO	formaldehyde
HD	heavy-duty
Hg	mercury
HVO	hydrotreated vegetable oil
ICE	internal combustion engine
IMEP	indicated mean effective pressure
$IMEP_G$	gross indicated mean effective pressure
IRD	infrared detector
IS	indicated specific
LCA	life-cycle assessment
LD	light-duty
LR	linear regression
LTC	low temperature combustion
MP	mixing period
MS	mass spectrometry
MSS	micro-soot sensor
NH_3	ammonia

NMHC	non-methane hydrocarbons
NMOG	non-methane organic gases
N_2O	nitrous oxide
NO	nitric oxide
NO_2	nitrogen dioxide
NOx	nitrogen oxides
O_{2in}	intake oxygen concentration
O_3	ozone
OP	operating point
P	phosphorus
PAH	polycyclic aromatic hydrocarbon
PAM	potential aerosol mass
Pd	palladium
PM	particulate matter
$PM_{0.1}$	particulate matter with an aerodynamic diameter less than 100 nm
$PM_{1.0}$	particulate matter with an aerodynamic diameter less than 1 μm
$PM_{2.5}$	particulate matter with an aerodynamic diameter less than 2.5 μm
PM_{10}	particulate matter with an aerodynamic diameter less than 10 μm
PMD	paramagnetic detector
PMP	Particle Measurement Program
PN	particle number
PN_{10}	total number of solid particles that have a diameter larger or equal than 10 nm
PN_{23}	total number of solid particles that have a diameter larger or equal than 23 nm
POA	primary organic aerosol
PPC	partially premixed combustion
P_{rail}	fuel injection pressure
Pt	platinum
Q_{LHV}	lower heating value
rBC	refractory black carbon

r_c	geometrical compression ratio
RCF	recycled carbon fuel
RFONBO	renewable fuel of non-biological origin
RME	rapeseed oil methyl ester
RoHR	rate of heat release
RON	research octane number
S	sulfur
SCR	selective catalytic reduction
SDD	silicon drift detector
SDG	sustainable development goal
SO_2	sulfur dioxide
SO_3	sulfur trioxide
SOA	secondary organic aerosol
SOC	start of combustion (CA5), the crank angle at which 5% of the charge has been consumed
SOI	start of injection
SP-AMS	soot-particle aerosol mass spectrometry
TDC	top dead center
TEM	transmission electron microscopy
THC	total hydrocarbons
TPNC	total particle number count
VOC	volatile organic compound
WHSC	world harmonized stationary cycle
WHTC	world harmonized transient cycle
XPI	high-pressure injection
Zn	zinc
λ	lambda, the ratio between the air-fuel ratio and the stoichiometric air-fuel ratio for the given fuel, $\left(\frac{A}{F}\right)/\left(\frac{A}{F}\right)_S$

1 Transportation and the Earth

Transportation is the backbone of every society and their progress. Mainly due to use of fossil fuels, this comes at a high cost for the Earth, but also for human health because of harmful local emissions. This PhD thesis is a compilation of studies focusing on heavy-duty transportation and its prime mover, the compression-ignition internal combustion engine. The possibility to replace fossil diesel fuel with a variety of renewable fuels is discussed throughout the thesis. Moreover, the experimental results on the local emissions of a truck engine operating on these alternative fuels are presented in Chapter 5.

1.1 The importance of sustainable transportation

Encyclopaedia Britannica provides a comprehensive definition of transportation declaring it a vital part of the modern society:

> Transportation, the movement of goods and persons from place to place and the various means by which such movement is accomplished. The growth of the ability–and the need–to transport large quantities of goods or numbers of people over long distances at high speeds in comfort and safety has been an index of civilization and in particular of technological progress. [1]

The 2030 Agenda for Sustainable Development, adopted by all United Nations Member States in 2015, provides a shared strategy for peace and prosperity for people and the planet, now and into the future [2]. It is based on the 17 Sustainable Development Goals (SDGs) consisting of 169 targets and 230 indicators which are an urgent call for action by all countries in a global partnership from now to 2030. They recognize that ending poverty and other deprivations must go hand-in-hand with actions that improve health and education, reduce inequality, and promote economic growth, all while tackling climate change and working to preserve the oceans and forests.

Sustainable transportation is not needed solely for its own sake, but rather as an important enabler to achieve the results defined in a large number of SDGs. Paragraph 27 of this broad policy agenda states that strong economic foundations for all countries will be built by providing sustainable transport systems, along with

universal access to affordable, reliable, sustainable and modern energy services, a quality and resilient infrastructure, and other policies that increase productive capacities [2].

1 NO POVERTY	1.4. ...ensure that all men and women..have access to basic services 1.5. ...reduce their exposure and vulnerability to climate-related extreme events
2 ZERO HUNGER	2.1. ...access to food all year round 2.a. ...increase investment..in rural infrastructure
3 GOOD HEALTH AND WELL-BEING	3.6. ...halve the number of global deaths and injuries from road traffic accidents 3.9. ...reduce the number of deaths from..hazardous chemicals and air pollution
4 QUALITY EDUCATION	4.3. ...ensure equal access for all women and men to..education
6 CLEAN WATER AND SANITATION	6.1. ...achieve universal and equitable access to safe and affordable drinking water for all
7 AFFORDABLE AND CLEAN ENERGY	7.3. ...improvement in energy efficiency
8 DECENT WORK AND ECONOMIC GROWTH	8.8. Protect labour rights and promote safe and secure working environment for all workers.
9 INDUSTRY, INNOVATION AND INFRASTRUCTURE	9.1. Develop quality, reliable, sustainable and resilient infrastructure, including regional and transborder infrastructure.
11 SUSTAINABLE CITIES AND COMMUNITIES	11.2. Provide access to safe, affordable, accessible and sustainable transport systems for all.
12 RESPONSIBLE CONSUMPTION AND PRODUCTION	12.3. ...reduce food losses along production and supply chains 12.c. ...fuel subsidies 12.4. ...achieve the environmentally sound management of chemicals
13 CLIMATE ACTION	13.1. Strengthen resilience and adaptive capacity to climate-related hazards 13.3./13.a. Climate Change Mitigation
14 LIFE BELOW WATER	14.1. ...prevent and significantly reduce marine pollution of all kinds, in particular from land-based activities
17 PARTNERSHIPS FOR THE GOALS	17.5. Adopt and implement investment promotion regimes. 17.11. Significantly increase the exports of developing countries. 17.17. Encourage and promote public-private partnerships.

Figure 1. SDGs relevant for the sustainable transportation [2], icons from [3].

The SDG targets directly or indirectly related to transportation are highlighted in Figure 1. They are guiding lights of this PhD thesis since they will be relevant even beyond year 2030. The starting point are the requirements that transportation of people and delivery of supplies should become sustainable and available to everyone. Despite transportation being important for the development and prosperity of people on this planet, if not controlled, its emissions can have detrimental effect on the climate and human health. Therefore, improved air quality and reduced negative health impact of emissions from transportation, as well as climate change mitigation are also crucial aspects to which the thesis contributes. When it comes to renewable fuels, apart from the transportation, they can also be used in power generation engines. Thus, this PhD thesis provides the knowledge that may also be beneficial for sustainable energy production in remote areas away from the electricity grid.

1.2 Fuels as a problem for, and solution to, global warming

1.2.1 Problem

Greenhouse gases (GHGs) are a natural part of the atmosphere. Unfortunately, the portion of the long-lived GHGs emitted as a result of human activity is too high as it affects the energy balance of the Earth, causing warming of the atmosphere [4]. Anthropological GHGs consist of mainly carbon dioxide (CO_2) at 55–60%, but also methane (CH_4), and nitrous oxide (N_2O). Black carbon (BC), a component of particulate matter (PM), also known as soot or a solid particle, is a short-lived climate pollutant, and the largest contributor to climate change together with GHGs [5].

In order to combat climate change, the majority of the countries (ca. 70%) in the world have committed to carbon neutrality latest by year 2050 [6]. The problem of global warming must be addressed globally and will need an assortment of technical and interdisciplinary solutions, as well as changed behaviors and policies that encourage producing less waste and using less resources.

Transportation accounts for approximately one sixth of GHG emissions globally, including direct emissions from burning fossil fuels to power transport activities, but excluding emissions from the manufacturing of motor vehicles or other transport equipment. Indirect emissions from electricity used in electric vehicles are also included in this number [7]. The portion of global CO_2 emissions from transportation which comes from internal combustion engine (ICE) powered road

vehicles was 74.5% in 2018 [8]. Heavy-duty (HD) trucks are responsible for almost 30% of global transportation emissions [8].

Heavy-duty vehicles are usually powered by a direct injection compression ignition (DICI) diesel fueled ICE, and similar engines are found in buses, trains, ships, farming and construction equipment, military vehicles or used as stationary emergency power generators [9]. They are renowned for their high efficiency, durability and high torque output, and therefore are an important propulsion technology for HD transportation. They have the potential to keep an important place in the transition to sustainable HD transportation, as it will be shown in the following chapters of this thesis. According to the Swedish Traffic Analysis Office, the dominating fuel type for heavy-duty trucks in Sweden is diesel [10], and most likely, the same trend will continue until at least the year 2030 [11], see Figure 2. When fossil diesel is used in HD DICI, PM is formed from incomplete combustion, and a large amount of fossil CO_2 is emitted.
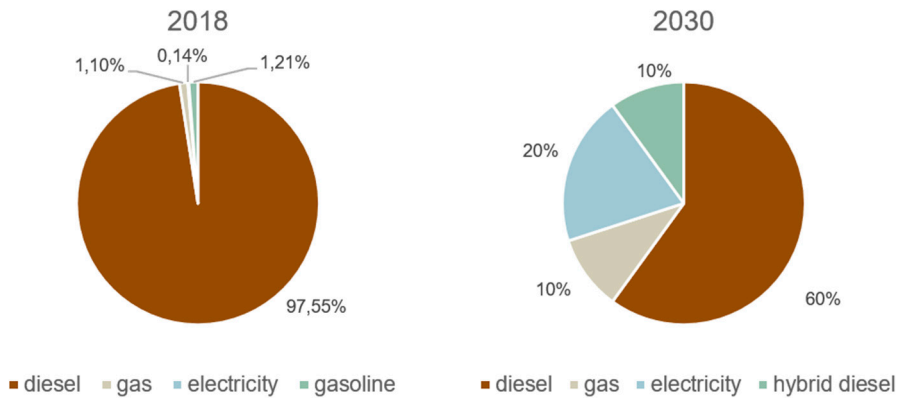
Figure 2. Distribution of heavy-duty truck fuels in Sweden in the years 2018 (left) and 2030 (right), data obtained from [10] and [11], respectively.

1.2.2   Solution

There is not a single solution that can defossilize transportation, but when it comes to the heavy-duty sector, the most straightforward way to go is to exchange fossil diesel fuel for a diesel-like fuel of non-fossil origin.

These alternative fuels can include gaseous fuels, such as hydrogen, biomethane, and propane; liquid biofuels, such as alcohols (methanol, ethanol and butanol); diesel-like vegetable and waste-derived oils; or fossil fuels that are less CO_2-intensive than the fuels that they replace. They can be used in a dedicated engine that runs on a single fuel, or mixed with other fuels including fossil gasoline or diesel, such as in flexible fuel vehicles (FFVs). In order to avoid creating additional

sources of GHG emissions as unintended consequences of solving the primary problem of transportation decarbonization, we need to adopt a holistic view of the mobility sector to understand the complexity, interdependencies, and impacts of the whole system in order to make a real progress [12]. The use of life cycle assessment (LCA), including, inter alia, the analysis of the raw materials collection, manufacturing, transport and distribution, usage, re-usage, maintenance, recycling of materials and final disposal or destruction [13], is needed to provide knowledge about the true environmental impacts of transportation systems so that effective emission reduction measures can be defined [14]. Besides, regulations have never been so important as today. Policymakers must focus on endgame results, while the science-based approach should ensure proper strategic decisions.

1.2.2.1 Electrification

Electrification is commonly seen as a way to be pursued in the energy transition. However, battery size and weight are the most limiting factors in heavy-duty electrification, since they affect the payload significantly. Other challenges are high price and short driving range. Materials availability is a separate topic to be addressed due to unethical mining of rare battery minerals [15], which is hopefully going to end with the support of the initiatives for the socially responsible and environmentally sustainable battery industry [16]. As researchers and engineers work on solutions, battery electric vehicles (BEVs) prices are decreasing and battery range is getting longer. There are plans for electric road systems (ERSs) to be built in future [17], and by allowing for more frequent charging, the battery size (and, thus, its cost, weight, and volume) may get reduced, or its lifetime may be extended due to less aggressive cycling [18]. Such a scenario may, however, result in higher overall energy consumption if the drivers decide to alter their routes to use the ERS, thus avoiding stopping for charging [18].

1.2.2.2 Hydrogen in ICEs

Hydrogen combustion engines and hydrogen fuel cells are receiving increased interest in the heavy-duty sector. The biggest advantage of hydrogen is CO_2-free combustion. In addition to the exhaust gas components, water, water vapor, and NOx emissions are the major emissions that can be produced from hydrogen ICEs. Since hydrogen fuel is carbon-free, no soot emissions are expected. Depending on engine hardware design, a very low amount of lubrication oil particles may participate in combustion, e.g. from piston rings (see [19]), or unburnt oil may escape the cylinder [20], which can produce a very low amount of unburned hydrocarbon emissions and particulate matter. In order for hydrogen vehicles to become commercially feasible, challenging tasks in hydrogen production, distribution and storage have to be addressed [21]. Hydrogen fueled powertrains can be seen as an interim solution for many applications for as long as alternative (electrified) powertrains are not available or feasible [22].

1.2.2.3 Renewable liquid fuels – biofuels

In contrast to electricity and hydrogen energy resources, biofuels can be in liquid form, which is essential for the current vehicles that can take full advantage of this efficient way of storing and distributing energy [23].

Biofuels are classified into four generations according to the type of the feedstock used for their production [24], as shown in Figure 3. First-generation (1G) biofuels are made of edible biomass, which makes them a part of the food-feed-fuel competition. Apart from biomass and land, biofuels also compete with food and feed production for water, capital and labor [25]. Second-generation (2G) biofuels use non-edible biomass, but there are still limitations related to the cost-effectiveness involved in scaling the production to a commercial level. Third-generation (3G) biofuels use microorganisms, like algae, that can use a diverse array of carbon sources as feedstock. A downside is that algae, even when grown in waste water, require large amounts of water and fertilizer (nitrogen and phosphorus) to grow. As a consequence, the use of algae-based biofuel may not result in any GHG emission savings compared to fossil fuels [26]. It also means the cost of algae-based biofuel is much higher than fuel from other sources. The definition of the 3G biofuels is being extended to utilization of CO_2 as feedstock [27][28][29]. Fourth-generation (4G) biofuels focus on modifying these microorganisms genetically to achieve a preferable hydrogen to carbon yield along with creating an artificial carbon sink to eliminate or minimize carbon emissions [30]. The fourth generation of biofuels is still in early development stages [31].
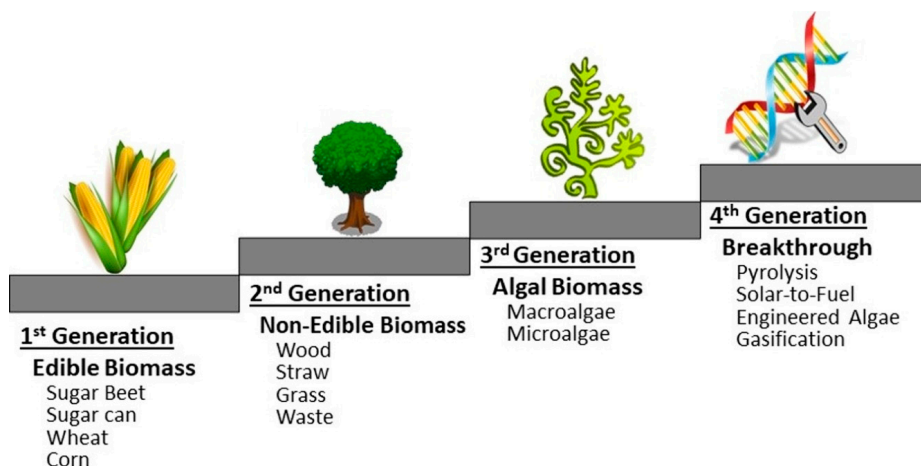
Figure 3. Generations of biofuels feedstock, reprinted from [24] with permission.

The following sections about fatty acid methyl ester (FAME), rapeseed oil methyl ester (RME), and hydrotreated vegetable oil (HVO) fuels are based on work in

Paper 1 and Paper 3, whereas the sections about E85, ethanol and methanol are developed from work in Paper 2 and Paper 4.

Fatty acid methyl ester fuels, usually called biodiesel, can be produced from primary vegetable oils such as soy, palm, coconut, or sunflower oil, etc., and therefore belong to 1G biofuels made from edible biomass. Rapeseed oil methyl ester is made by esterification of rapeseed oil by use of methanol. Most vehicles with DICI engines in Europe currently use low level blends of FAME in diesel, i.e. B5 or B7. Increasing of the added fractions of oxygen-containing FAME biodiesel fuels, or other diesel-like fuels produced from renewable biomass resources, into fossil diesel is currently encouraged in order to reduce GHG emissions [32], and reaches as high levels as over 50% in some diesel fuels available in Sweden [33]. The advantages of RME combustion are significantly reduced emissions of unburned hydrocarbon (HC), carbon monoxide (CO) and particulate matter [34]. However, pure RME still cannot directly replace fossil diesel because it can produce higher NOx if used as a drop-in fuel, i.e. without changing the original diesel engine settings. NOx can actually go down, too [35]. RME can have detrimental effects on fuel injection systems [36]. Also, RME has higher density and 13.6% lower energy density than fossil diesel, as well as poor cold flow properties [37] and oxidation stability, but it possesses good lubricity. Further, the quality of FAME is dependent on the properties of the feedstock used, thus limiting the choice of feedstock suitable for cold climate regions [38].

On the other hand, high levels of hydrotreated vegetable oil fuel can be blended with fossil diesel without affecting the engine performance. HVO can also be used neat and in that case, it is called renewable diesel. Fuel properties of HVO are close to fossil diesel fuel and therefore, their logistics, storage, and combustion properties are similar [38][39]. The HVO production process involves removal of oxygen from the triglycerides by the use of hydrogen. Additionally, the HVO properties are not as sensitive to different feedstocks of vegetable oil as in the case of biodiesel. Even though edible oils are the main feedstock for HVO production, non-edible oils, such as pongamia, can also be used, as well as used frying oil, fat residues from the meat and fish industry, and technical corn oil (a residue from ethanol production). That kind of HVO can be classified as a 2G biofuel. The lubricity of HVO is very low due to the absence of sulfur and oxygen compounds in the fuel [40] and it thus needs friction modifying additives. Due to lower density resulting from the aliphatic nature of the compounds [41], as opposed to fossil diesel containing aromatic hydrocarbons, HVO has ~4% lower volumetric heating value than fossil diesel. Because the energy content of HVO is slightly higher per mass, the effect of lower density is partly compensated [40]. Its cetane number, or tendency to autoignite, is very high. Despite the cetane number being regarded as a quality indicator of diesel fuels, the high difference between the cetane numbers of diesel and HVO could potentially require changes in the engine control to compensate for the fuel igniting earlier in the cycle [42]. Due to the higher paraffinic character of HVO, its cold flow

properties might also be worse than those of a winter diesel fuel, although this depends highly on the oil feedstock [43][44] and on the reaction conditions which may lead to a certain yield of triglycerides [44].

Both HVO and FAME-type fuels can significantly reduce PM, HC, and CO emissions in diesel exhaust [45][46] and change the particle size distribution and soot nanostructure [34][47] in comparison to fossil diesel. Switching to these renewable and sustainable fuels has the proven potential to reduce GHG emissions [48] and improve the air quality with the existing fleets of vehicles, especially of those without an exhaust aftertreatment system (EATS) [49]. A recent study shows that the use of 100% renewable diesel can achieve lifecycle GHG reductions at a level comparable to the use of BEVs, allowing for faster decarbonization of existing fleets in the nearest future [50]. However, there is little to no knowledge about the composition (physical and chemical properties) and origin (from fuel, lube oil, or combustion) of organic aerosol emitted from combustion of HVO and RME.

Alcohol blends can also be used in different ways in ICEs, as summarized in [51]. During the DICI process, alcohols do not form intermediate soot precursors due to their simple molecular structure [52], so the PM emissions are reduced to ultralow levels compared to diesel fuel, without a need for EATSs. NOx emissions are also reduced, whereas HC emissions can either increase or decrease. The main alcohols that can be used to achieve this are methanol and ethanol. The benefits of using low-sooting ethanol fuels in DICI engines were initially presented in [53]. A recent study [54] proposes that wet ethanol and methanol can be used interchangeably in an engine designed to accept high-cooling potential alcohol fuels, meaning that it can operate on wet ethanol, methanol, or their blends, depending on local availability, making it unnecessary to choose one fuel over the other as a replacement fuel in internal combustion engines.

E85 is another alcohol-based fuel, consisting of up to 85% anhydrous ethanol by volume mixed with gasoline without aromatics; the composition is approximately 85% ethanol and 15% gasoline in the summer blend, and 75% ethanol and 25% gasoline in the winter blend. It is commonly used in spark ignition engines produced to operate on ethanol in FFVs or gasoline engines converted for ethanol operation. Several models of light vehicles running on E85 have been present on the European market. The infrastructure for production, delivery and sale of E85 is well developed in the USA, France, Sweden, and a few other European countries, making E85 fuel commercially available there. The nominally 15% by volume gasoline in the blend serves to denature the alcohol to prevent ingestion, to provide a more ignitable mixture (which is particularly important at low temperatures) and also to provide a more visible flame in case of a vehicle fire [23]. A report by the Swedish Energy Agency [55] which includes a well-to-wheel analysis of several liquid fuels and electricity, shows that GHG emissions per energy content during the fuel lifecycle are reduced by 36% when E85 is used instead of fossil diesel. The ethanol in E85 sold in Sweden is 81% of fossil-free origin. A possibility to additionally reduce the

GHG emissions lies in replacing the gasoline with biogasoline, i.e. renewable gasoline that is a side product of renewable diesel production [56] or bio-based gasoline, made of residuals from the forest industry, hemicellulose and cellulose based sugars. E85 is a fuel which combines the properties of the two high RON fuels: ethanol [57] and gasoline [58], making it a good candidate for a DICI fuel burning in low temperature combustion (LTC) mode [59][60].

First-generation bioethanol is traditionally made through biological processes, such as fermentation of biomass, usually from sugarcane, sugar beets, grains or corn. New production processes for 2G ethanol have been developed, including pre-treatment, enzymatic hydrolysis and fermentation. They reuse waste products from other industries, such as lignocellulose residues (pulp and paper). In integrated bio-refineries, the total lignocellulosic biomass is valorized by producing valuable specialty chemicals alongside 2G ethanol. The energy platforms for burning lignocellulose residues in boilers for co-generation of heat and power (CHP) are already well-established and can be used in 2G ethanol production as well [61].

As a fuel used in ICEs, methanol has chemical and physical fuel properties similar to ethanol. Methanol is conventionally made from fossil sources, usually either by steam reformation or from coal with a significant fossil CO_2 impact [23]. The developments in biomass gasification have enabled the usage of a variety of biomass feedstocks to produce syngas, which in turn can be converted to biomethanol [31], making it either a 1G or 2G biofuel. Methanol can be made from anything carbonaceous, via chemical processes which synthesize the molecule from carbon, oxygen and hydrogen atoms [23], making it fall either into a group of 3G biofuels or electrofuels. Since chemical processes are generally significantly more rapid than biological ones, this has the potential to increase production rates [62][63]. As a consequence, methanol production is potentially more easily scalable and could also be coproduced in bioethanol plants in order to increase the overall energy yield from the used feedstock [64].

A drawback is that it is difficult to ignite these light alcohols in a DICI engine. Their low cetane numbers make them unsuitable for CI engines because of their poor auto-ignition qualities, which is most pronounced for methanol. The problem comes from its high octane number, low lower heating value and high heat of vaporization, which results in high amount of heat being needed to ignite methanol [65].

New forms of fuel, recycled carbon fuels (RCFs) and renewable fuels of non-biological origin (RFONBOs), are categories of alternative fuels incentivized by the European Union's recast Renewable Energy Directive adopted in 2018 (RED II) [66]. Specifically, for RCFs, REDII analyzes the climate impact of bacterial fermentation of CO in industrial off-gases and liquid fuels from plastic waste, and for RFONBO, the potential for a synthetic fuel from renewable electricity pathway. There are, however, studies indicating that not all pathways for these two fuels will result in net climate benefits [67].

1.2.2.4   *Slowing down the climate change and further improving air quality*

The new revision of the EU Renewable Energy Directive (RED III) is expected to be adopted by the end of 2022 and it will emphasize the critical role of sustainable biodiesel to reach the EU climate objectives [68]. Moreover, it will require urgent and increased emission cuts for the transportation sector with a 16% GHG intensity reduction target, coupled with a 45% overall renewables target. Since electrification is not yet viable over the whole transportation sector, the use of renewable and low-carbon fuels, including hydrogen, is promoted [69]. This is a highly needed plan which will require all renewable energy sources to contribute in order to reach these ambitious targets.

Applied on modern vehicles, emission regulations have led to significantly reduced emissions from combustion engines. Currently, Euro 6 for light-duty (LD) vehicles, and Euro VI for HD are in force, and they control particle emissions by a PM mass and a solid particle number (SPN) limit. There are concerns that the SPN limit excludes certain relevant particulate species, and several semi-volatile particle emissions can be an order of magnitude higher than SPN emission levels [70]. Particles of size below 23 nm are currently not included in these emission regulations, but their monitoring is highly recommended [71] and will be included in the future legislations down to the size of 10 nm.

Table 1. European (indicated specific) emissions standard Euro VI for heavy-duty diesel engines in stationary (WHSC) and transient (WHTC) test cycles, compared to proposed Euro 7 hot and cold emission limits for heavy-duty engines.

	Euro VI		Euro 7		
	WHSC	WHTC	cold emissions (WHTCcold)	hot emissions (WHTChot)	emissions budget for trips shorter than 3 lenghts of WHTC
CO [mg/kWh]	1500	4000	3500	200	2700
PM [mg/kWh]	10	10	12	8	10
PN_{23} [#/kWh]	8×10^{11}	6×10^{11}	–	–	–
PN_{10} [#/kWh]	–	–	5×10^{11}	2×10^{11}	3×10^{11}
NOx [mg/kWh]	400	460	350	90	150
NH_3 [ppm]	10	10	–	–	–
NH_3 [mg/kWh]	–	–	65	65	70
HC [mg/kWh]	130	160	–	–	–
CH_4 [mg/kWh]	–	–	500	350	500
NMOG [mg/kWh]	–	–	200	50	75
HCHO [mg/kWh]	–	–	30	30	–
N_2O [mg/kWh]	–	–	160	100	140

Simultaneously, there have been intense discussions on the formulation of the new pollutant emission standard Euro 7. This emission standard expands the definition of pollutants, including for example formaldehyde (HCHO), to reflect the increased use of renewable fuels, and dividing total HC into more specific groups.

The current emission limits given by the Euro VI emission standards for HD vehicles which were introduced in Europe in 2014 [72], are compared to the proposal of Euro 7 which will apply from July 2025 [73], in Table 1. For definitions of pollutants and measurement techniques see [74].

While effects of renewable fuels on GHG reduction start to become reasonably well understood, there is less data on the characteristics of pollutant emissions from combustion of renewable fuels, both primary and secondary PM, since they may differ from fossil diesel emissions [49][75][76]. Also, different combustion modes can further change the exhaust composition. Therefore, understanding both effects of the new fuels, as well as new combustion concepts, is crucial for designing the systems for emission reduction and for understanding the health effects of the emitted pollutants.

The main motivation for improving the air quality is above all the devastating fact that every year 6,700 people die only in Sweden [77], and 238,000 across the Europe [78], just from breathing air containing fine particles. The association between fine particles and mortality, despite the air quality improvements in the recent years, continues to be the major health problem according the WHO Air Quality Guidelines [79].

2 Direct injection compression ignition engines

A brief overview of the combustion in direct injection compression ignition engines at the start of this chapter is followed by a review of the gaseous and particulate matter emissions from these engines, as well as primary and secondary organic aerosol in the atmosphere. Finally, a discussion on emission reduction techniques, including exhaust gas recirculation, low temperature combustion and exhaust aftertreatment systems, is presented. The knowledge gaps are highlighted throughout this chapter, and will be summarized in the next chapter in form of the thesis statement and aims.

2.1 Conventional diesel combustion

In a compression ignition internal combustion engine, also known as a diesel engine, the intake air is compressed to high pressure, or first mixed with residual combustion gases from the exhaust, if exhaust gas recirculation (EGR) is used, and then compressed. Diesel fuel is then directly injected into the combustion chamber at a high pressure and atomized to small droplets, vaporized and mixed with the hot charge. When the resulting in-cylinder charge temperature becomes high enough, the injected low ignition resistance fuel (diesel or a diesel-like fuel) gets ignited. According to a conceptual direct injection diesel spray model proposed in [80], the core of the spray contains rich mixture and the soot is formed there. Full oxidation of the fuel occurs in the diffusion flame at the periphery of the spray around stochiometric conditions. That is the location where the bulk of heat is released, soot is oxidized and thermal NOx is produced, see Figure 4. The combustion speed is controlled by the mixing of fuel and the cylinder charge and ends when all the fuel is consumed. This process is called conventional diesel combustion (CDC). The products of the combustion, also called diesel exhaust, are emitted from the engine, through a line of engine aftertreatment system components. These tailpipe emissions are then let out into the atmosphere.
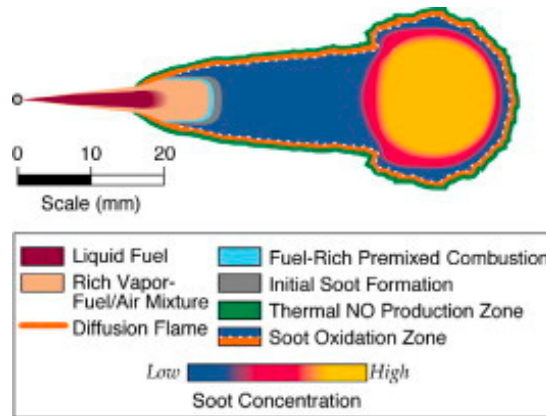
Figure 4. Conceptual schematic of mixing controlled combustion, reprinted from [80] with permission.

Injection timing, injection pressure and the composition, amount and ratio of fuel, air and EGR can control the start of combustion (SOC), speed of combustion, the torque and tailpipe emissions that the engine produces.

2.2 Gaseous emissions

The regulated gaseous pollutant emissions generated from fuel combustion in internal combustion engines include nitrogen oxides (NO and NO_2, together called NOx), hydrocarbon (HC), also called volatile organic compounds (VOCs) or non-methane hydrocarbon (NMHC), and carbon monoxide (CO) [81].

When released into the atmosphere, unburnt HC reacts with NOx in the presence of sunlight, to form ozone (O_3) which is a main component of photochemical smog. Heat from ultraviolet light provides the activation energy required to initiate the reaction. On the other hand, CO causes direct harmful health effects by reducing oxygen delivery to the body's organs and tissues, and affecting cell operation. Exposure to even low levels of CO, which may occur in cities with dense traffic [82], is dangerous for those who suffer from heart disease, and can cause chest pain, or contribute to other cardiovascular effects with repeated exposures [83][84]. Even healthy people who breathe in medium levels of CO, present for example in air pockets like parking lots [82], can experience vision problems, reduced ability to work or learn, reduced manual abilities, and difficulties performing complex tasks. At high levels, CO is poisonous and can cause unconsciousness and eventually death. The levels of CO can be especially high in traffic tunnels due to their enclosed structure and during rush traffic in developing countries [85].

36

The overview of the current (Euro VI) and future (Euro 7) European emission legislations for heavy-duty vehicles is given at the end of Chapter 1 of the thesis.

2.3 Diesel particulate matter and aerosols

Aerosol particles in the atmosphere have adverse effects on air quality. The smallest of them easily penetrate the human pulmonary system and have been linked to severe short- and long-term health impacts, such as asthma, cardiopulmonary diseases, and lung cancer [86]. Since some aerosols mainly scatter solar radiation back into space and thereby cool the climate, while others, like BC, contribute to warming, they present one of the largest uncertainties in climate modelling and prediction. They also affect the climate indirectly through their role as cloud condensation nuclei (CCN) and ice-nuclei [87].

In the automotive field, the term *particulate matter* is used for the primary particles from vehicle exhaust collected on a flow-through filter under specific conditions, and the term *particle* for aerosol particles measured while airborne (suspended matter).

Although particle characterization techniques have significantly developed during recent years, enabling online measurements of even the smallest nanoparticles, the mass of these smallest particles is, however, almost negligible despite the large number concentrations [88]. In the Particle Measurement Program (PMP) protocol from EU, solid particles refer to those particles that survive heating to 300°C in the measurement set-up prior to particle counting. Current legislations mandate measurements of particle mass and solid particle number. They should, however, be revised to include total particle number count (TPNC) after the tailpipe, since both number and mass are important to understand various aspects of the climate and health effects of atmospheric aerosols [89][90]. Even though the technology to measure TPNC exists, it is yet to be strictly defined how it will be implemented in a regulatory framework [70].

The three mains factors influencing PM toxicity are chemical composition (e.g. the organic fraction), surface area, and the place of deposition in the respiratory tract upon inhalation. The deposited fraction primarily depends on the size, but also shape and density of the aerosol particles [91]. According to the size of the largest aerodynamic diameter in the group, PM can be classified as coarse, fine, submicron and ultrafine, see Table 2. A simple example of comparison is that one coarse PM_{10} particle has approximately the same mass as one million ultrafine $PM_{0.1}$ particles, but their health impacts are completely different. PM_{10} are mostly deposited in the upper airways, where they stay until removed by clearance mechanisms [91]. $PM_{2.5}$ can also travel deep into the respiratory tract, reaching the lungs, and due to their large surface areas, they can carry toxic material [92]. $PM_{0.1}$ are, however, deposited

in the alveolar region of lungs that have weak nanoparticle elimination mechanisms. Peaks in deposition at 20 nm and 1.5 μm are observed, since the alveolar region cannot eliminate these smallest particles with high surface area and number concentrations [93]. They may translocate beyond the lung and cause adverse effects on the central nervous system, extrapulmonary organs and cause dysfunction of blood vessels causing negative cardiac effects [94][95].

Table 2. Size classification of PM.
*Ultrafine particles do not have a clear definition, their lower cut point is not defined [96], but can be assumed to be 2–10 nm determined by the capability of the particle counter [97].

name	symbol	size (less than)	
		[μm]	[nm]
coarse	PM_{10}	10	10000
fine	$PM_{2.5}$	2.5	2500
submicron/fine	$PM_{1.0}$	1	1000
ultrafine*	$PM_{0.1}$	0.1	100
nano	$PM_{0.05}$	0.05	50

The tailpipe exhaust of a vehicle consists of solid primary non-volatile particles (soot, black carbon), which represent a good adsorption surface for the hundreds of compounds produced after incomplete combustion in diesel engines, such as gaseous emissions at high exhaust temperatures, and trace metals. Aerosol precursors (e.g., sulfuric acid, hydrocarbons) [98][99] are in the gas phase at high temperatures as semi-volatiles [70]. A subgroup of potentially toxic, mutagenic and carcinogenic hydrocarbons found in the emissions, polycyclic aromatic hydrocarbons (PAHs) [100][101], can originate from the combustion, but also from unburned diesel fuel, lubricating oil and the pyrosynthesis of low molecular weight polyaromatics. PAHs with two or three aromatic rings are often detected in the vapor phase, whereas those with between four and seven fused rings are found mostly in the particle phase [102]. A comprehensive explanation of the soot formation processes and soot composition is reported in [103].

Typically, diesel PM consists of two main modes in the size distribution, accumulation and nucleation modes, see Figure 5. The modes mainly depend on the engine, fuel, combustion strategy, and aftertreatment devices [88][104][105]. Soot or accumulation mode particles are measured at the tailpipe with a mean diameter size >50 nm [106], or around 30–100 nm, as defined in [107][108], and they consist of many spherical primary particles of elemental carbon [109] with attached fuel and lubrication oil components [110], and particle-bound PAHs [111][112][113][114]. Additionally, PM can have one solid core or nano-mode with a mean size below 10–15 nm [115][116][117], or two nano-modes (one from lubricant and one from fuel) [118]. The nano-mode consists of amorphous

carbonaceous compounds, PAHs, or metallic ash from fuel or lubricant [119][120][121][122].
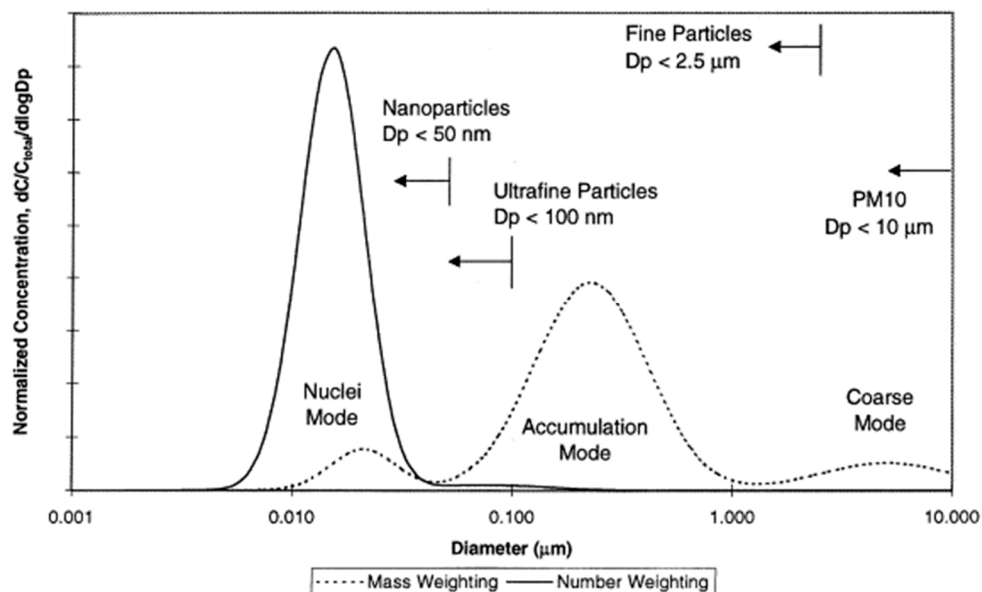
Figure 5. Typical engine exhaust size distribution, by both mass and number weighting, reprinted from [107] with permission.

Nanoparticles are emitted even when there is no combustion in the engine, i.e. during braking (motoring the engine) [49][123][124], and engine and aftertreatment wear particles may also be emitted [125], as well as coarse mode particles originating from the crankcase ventilation, wear, or soot re-entrainment [107][126].

Undiluted vehicle exhaust emissions in the tailpipe contain also a variety of different components which are in gaseous phase because of the high exhaust gas temperatures. These aerosol precursors, mainly VOCs and sulfuric acid, get diluted and cool down [127][128][129], and can consequently nucleate to form new nucleation mode particles, or alternatively condense on other particles, i.e. non-volatile core or accumulation mode [70]. Therefore, the fresh exhaust aerosol contains both the solid particles in the tailpipe (primary PM) and the particles newly formed within the seconds of mixing of the exhaust gas with ambient air [88][130]. The peak of the formed nucleation mode, in the absence of a solid core, lies at around 10 nm depending on the availability of the precursors [107][131][132][133]. Whether condensation or nucleation dominates depends on the availability of pre-existing particle surface area (condensation sink) [134] along with the dilution and cooling rate [97].

One of the identified research areas of importance for characterization of the health and environmental impacts of nanoparticles is understanding composition and sources of PM, their mechanisms of formation and transformation in the atmosphere [88].

A large fraction (~50%) of the submicron aerosol particle mass in the troposphere is a complex mixture of hundreds of different organic compounds [135][136]. Organic aerosol (OA) can either be primary organic aerosol (POA) directly emitted by different sources, including anthropogenic (transportation and combustion activities) and biogenic, or secondary organic aerosol (SOA) formed through chemical reactions in the atmosphere.

2.4 Secondary organic aerosol

The atmospheric secondary organic aerosol plays an important role in the global particulate matter budget, and its chemical composition determines critical properties that impact radiative forcing and human health [137].

Recent studies have shown that secondary PM from combustion engines consists mainly of organic compounds and ammonium nitrate [138][139]. Ammonium nitrate is detected mostly downstream major cities in winter time, forming when traffic NOx escapes after an inefficient selective catalytic reduction (SCR), then reacts to nitric acid, and finally meets an ammonia plume. An example is traffic exhaust from Benelux that passes over the fertilized farms in Denmark, before arriving to Sweden. Finally, the secondary PM formation can be significantly larger than the primary PM emission [139][140]. The contribution from vehicles to SOA can be higher than the primary aerosol they emit [139].

SOA is produced via secondary formation in the atmosphere (atmospheric aging) when the oxidation products of gas-phase volatile organics or gaseous hydrocarbon precursors undergo the gas-particle transfer through nucleation, condensation or heterogeneous and multiphase chemical reactions [137][141], as shown in Figure 6. The emissions of secondary PM precursors depend on fuel properties, as well as engine type, load and aftertreatment systems [49][75][138][142]. Both fuel and oil are significant sources of hydrocarbons emitted from diesel engines [143][144][145][146] and the emissions of secondary PM precursors depend on fuel properties [49][75][138][142], however lubrication oil has been proposed to dominate POA emissions [147][148] and have stronger influence on the SOA formation than the fuel composition [138][139][142][149]. This process is complicated since each VOC can undergo a number of atmospheric degradation processes to produce a range of oxidized products, which may or may not contribute to SOA formation and growth [137]. There is also a difference between processes controlling particle number and processes controlling particle mass; condensation

of vapors (sulfuric and nitric acids, ammonia, and secondary organics) onto existing particles may dominate particle mass without necessarily influencing particle number [150].

Organic Aerosol Morphologies

biphasic ⟶ homogeneous

water-rich phase

organic phase

emissions

vapor oxidation

0   0.4   0.8
Increasing oxidation state (O:C)
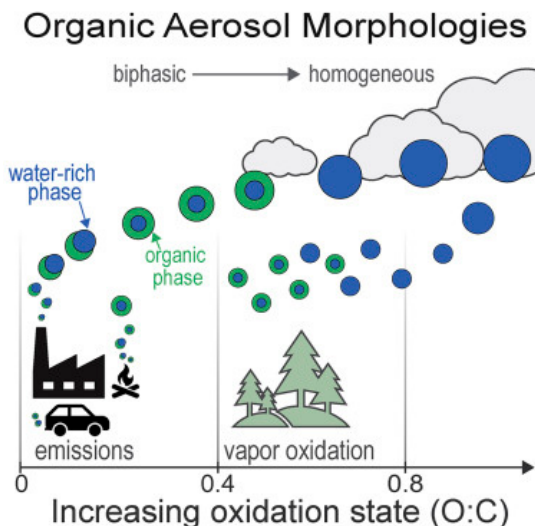
Figure 6. Evolution of the organic aerosol in the atmosphere. SOA forms from gas phase organics. Reprinted from [151] with permission.

A better understanding of semi-volatile compounds from vehicles is needed in order to estimate their contribution to secondary aerosol formation [70]. Also, in order to make more accurate climate models, a better understanding of the behavior of aerosols in the atmosphere is needed [152]. One way to obtain detailed information on the sources and components of organic aerosol is from statistical analyses of the mass spectral data [153][154], provided by mass spectrometry (MS), an analytical technique used to measure the mass-to-charge ratio of one or more molecular fragments present within a sample and determine their relative abundance. To interpret the results of these statistical methods, presented as a plot of intensity as a function of the mass-to-charge ratio, however, mass spectral signatures of various organic aerosol sources and components need to be known [153]. The source appointment of OA measured in the air can distinguish factors with specific temporal variation and mass spectral patterns [141].

In order to characterize the POA and SOA material, the oxidation state, i.e. O:C ratio, is defined as a parameter that is expected to be closely related to an organic molecule's polarity and hydrophilicity. These are important parameters that influence aerosol properties, such as the phase behaviour [151][155], SOA formation during approximately a week-long atmospheric residence period, or how SOA continues to age, increasing O:C, by oxidation reactions [156][157]. The O:C

ratio has the practical advantage that it can be readily measured for atmospheric POA and SOA using online aerosol mass spectrometry [158].

2.5 Emission reduction techniques

2.5.1 Active reduction

Exhaust gas recirculation and low temperature combustion are active ways of reducing emissions, as they affect the combustion and change the resulting composition of the emissions.

Because of high in-cylinder temperatures during combustion, diesel engines produce and emit high levels of NOx. Moreover, the composition of fossil diesel fuel is such that its combustion produces soot and high PM emissions.

In order to reduce NOx emissions, an internal combustion method called EGR was introduced. The fraction of recirculated exhaust mixed with fresh intake air controls the concentration of the available oxygen, and also decreases the combustion flame temperatures. When EGR further increases, the engine operation reaches zones with higher instabilities, increased unburned HC, CO and soot emissions, and even power losses [159][160][161]. The effects of EGR on the engine performance and legislated emissions have been well studied, however less is known about its effect on the chemical and physical properties of particles, possibly causing changes in toxicity. Choosing the right amount of EGR for a specific operating condition is important.

In CDC, the soot formation occurs in the fuel-rich zones, while the soot oxidation occurs at high-temperature near-stoichiometric reaction zones with entrainment of ambient air [80][162]. Contrastingly, formation of NOx emissions is inevitable in the high temperature zones where soot particles are burnt off, resulting in a trade-off between soot and NOx emissions, so-called NOx-soot trade-off. EGR or retardation of fuel injection timing can be used to reduce NOx emissions, reducing the temperatures and residence times that are necessary to burn off soot particles, which usually causes an increase in soot emissions [163].

Furthermore, low temperature combustion has attracted the attention of the research community and engine manufacturers because it showed that it is possible to simultaneously avoid soot formation and NOx formation [164], and thus avoid the NOx-soot trade-off. The local air-fuel mixture needs to be sufficiently lean in order to prevent soot formation, however not too lean so not to go under the ignitability limit. The combustion temperature needs to be sufficiently low to avoid the NOx formation zone, but high enough to achieve sufficient oxidation rates and thus avoid high CO and HC emissions. Lean mixture can be achieved by increasing the heat

capacity of the mixture by EGR dilution, or water injection, or by boosting the intake pressure and diluting the mixture with the excess of air [165][166][167].

Combining high levels of EGR with fuel injection in the last quarter of the compression stroke results in partially premixed combustion (PPC), which can be classified as LTC [168]. The use of fuel with high octane number results in longer premixing times during which more air gets entrained into the fuel jet before it ignites, so the local rich zones get suppressed and the soot formation is reduced [169][170][171]. With reduced combustion temperature, emissions of immature soot or PAHs may increase. These changed particle properties can affect the effects on health or the aftertreatment efficiency significantly. More research is needed in this area.

Light alcohols, methanol and ethanol, can be used as fuels in diesel engines. Since they are not producing high amounts of soot, the NOx-soot trade-off can be removed, and it is possible then to adjust the combustion mode, as well as the EGR levels for high efficiency and low NOx emissions.

2.5.2   Passive reduction

Once the pollutants are produced during the combustion and emitted as diesel exhaust, exhaust aftertreatment systems can be used to reduce multiple pollutants [172]. Understanding the properties of raw engine emissions contributes to the development and optimization of EATSs, such as diesel oxidation catalysts (DOCs), diesel particulate filters (DPFs) and selective catalytic reduction (SCR), which in their turn can alter the physical and chemical composition of PM [173][174]. The nanostructure of soot is especially important for the oxidation kinetics in the exhaust aftertreatment [175][176].

The introduction of DPFs has significantly reduced the concentration of primary particles in the exhaust gas of modern vehicles and working machines [177][178]. The main function of a DOC is to ensure the sufficient oxidation of the gas phase HC and CO, but also to remove the organic fraction of the exhaust PM while still in the gas phase [179][180]. It has been reported that the DOC can increase the SO_2 to SO_3 conversion and NH_3 emissions [181][182]. Regarding the precursor gases, a DOC reduces hydrocarbons, and NOx reduction aftertreatment decreases NOx levels [183]. Consequently, the secondary aerosol formation is reduced, and this is valid both for diesel and HVO [142], as well as for RME [49]. However, as mentioned in the previous chapter, the knowledge about both the sources of the emitted organic aerosol composition (fuel, lube oil, or combustion generated), and effects of renewable fuels in combination with EATSs, is still scarce.

3 Thesis statement and aims

Renewable fuels of different properties can potentially replace fossil diesel fuel in an existing HD DICI engine without compromising the engine performance or introducing a need for major hardware modifications which cannot be overcome by the existing technological solutions. The GHG emissions will be reduced by keeping the atmospheric carbon in a loop by growing new feedstock for biofuels, while the fossil carbon remains in the ground.

An important area in which the knowledge is lacking is composition and origin, as well as mechanisms of formation and transformation in the atmosphere, of primary and secondary PM, including organic aerosol, emitted from combustion of HVO, RME and light alcohols, without or with an EATS. Additionally, new combustion concepts, such as low temperature combustion and using EGR, can affect the chemical and physical properties of particles, possibly causing changes in toxicity due to immature soot or PAHs. The nanostructure of soot is especially important for the oxidation kinetics in the exhaust aftertreatment.

The overall aim of this PhD thesis is to investigate the effect of replacing fossil diesel fuel with renewable diesel-like and alcohol fuels on the local exhaust emissions of an HD DICI engine and its performance in low to mid load range within studied operating conditions.

The specific aims of the thesis are to:

1. Compare the particle size distribution from an HD DICI engine exhaust of the diesel-like fuel RME (Paper 1), as well as from ethanol and methanol (Paper 2), to that of fossil diesel.

2. Compare the nanostructure of soot from combustion of RME (Paper 1), and of methanol and ethanol (Paper 2), with that of fossil diesel.

3. Investigate whether PM emitted from an HD DICI engine utilizing less-sooting fuels (RME, HVO, methanol and ethanol) mostly originate from engine lubrication oil (Paper 1, Paper 2 and Paper 3).

4. Investigate how the diesel-like fuels RME and HVO affect OA and SOA composition, and assess if the organic fractions come from lubrication oil (Paper 3).

5. See the effect which a DOC has on OA and SOA in the exhaust from combustion of fossil diesel and HVO (Paper 3).

6. Determine the viability of the use of E85 fuel in an HD DICI engine, and model and study the influence of three parameters controlling the combustion processes on the engine behavior (Paper 4).

4 Methodology

The experiments described in this thesis were performed on a heavy-duty compression ignition engine with direct fuel injection, located in the Engine Lab at the Division for Combustion Engines at Lund University. Experiments presented in Paper 1 and Paper 2 were conducted on a single cylinder HD CI engine within the same measurement campaign in 2016. Results in Paper 3 were obtained on a different engine but of the same type and with practically identical test bench configuration in 2018. A year later, the experiments from Paper 4 were also done on the latter engine.

In Paper 1, gaseous emissions and physical and chemical properties of particulate matter were studied as a function of the used fuel, biodiesel and fossil diesel, and intake air oxygen concentration by the means of changing EGR levels.

In Paper 2, emitted particles from combustion of the light alcohols methanol and ethanol were analyzed and compared to the ones originating from fossil diesel fuel as a function of the engine load.

In Paper 3, organic aerosol and secondary organic aerosol emissions were studied as a function of the diesel-like fuel used and the use of the emission aftertreatment.

Paper 4 investigated the viability of E85 fuel in compression ignition engine and looked into the engine performance and emissions as a function of the fuel/air ratio, fuel injection pressure and combustion timing.

4.1 Experimental arrangements

4.1.1 Engine apparatus

The experiments were performed in a Scania D13 heavy-duty six-cylinder diesel engine modified in such a way that only one cylinder was operating while the other five were motored without compression. Figure 7 shows the schematic diagram of the experimental engine and surrounding setup. The specifications of the experimental engine and used injectors are given in Table 3.

The engine was connected to an electric motor (dynamometer) rotating at a constant 1200 rpm. It motored the engine during the start-up and switch-off phases, and kept the engine at a constant rotational speed when fired. A crank angle encoder was also connected to the engine in order to provide a relationship between the current position and the top dead center (TDC) in crank angle degrees (CAD).

The fuel was injected through a solenoid injector connected to a common rail and a high-pressure injection (XPI) fuel pump. The fuel supply system on this engine was designed for a Scania ED95 ethanol engine suited for operation with low-lubricity corrosive fuels. Both types of injectors listed in Table 3 were suitable for alcohol injection. The existing equipment was used and therefore the engine piston was of the standard stepped bowl shape with geometrical compression ratio (r_c) of 17.3:1.
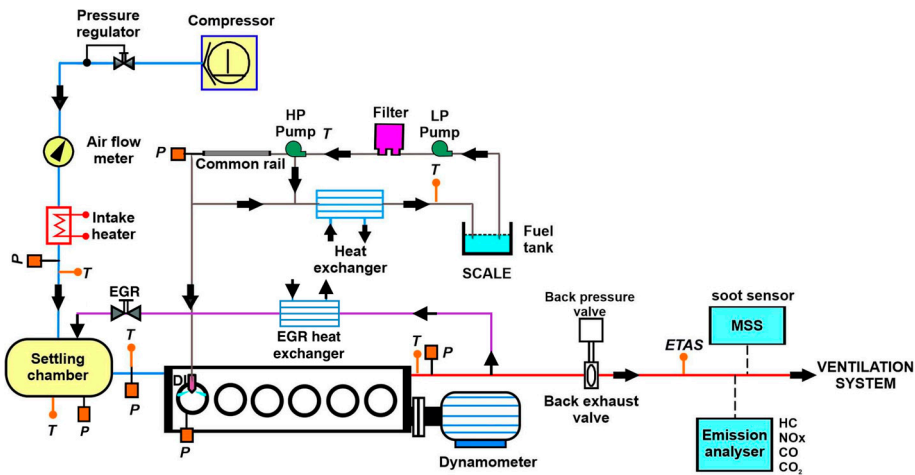
Figure 7. Schematic diagram of the experimental engine. The EGR loop was used in Paper 1 and Paper 3, whereas the EGR valve was sealed off in Paper 2 and Paper 4. Adapted from [184] with permission.

Table 3. Single cylinder engine specifications.

cylinders	originally six, operated on one (cylinder 6)	
displacement volume [cm³]	2124	
stroke [mm]	160	
bore [mm]	130	
connecting rod length [mm]	255	
geometrical r_c	17.3:1	
number of valves	4	
injector	Papers 1, 2 and 3	Paper 4
number or holes	10	12
spray angle [°]	148	120

The engine was supercharged with an external compressor providing pressurized oil-free dry air with a 7.5 kW heater located between the fresh air supply and intake manifold. The heater was either switched off or tuned to achieve the desired intake air temperature. The engine test rig was equipped with an adjustable EGR system which consisted of an EGR valve and an exhaust backpressure valve. The cooled, high-pressure EGR was introduced to the intake plenum for blending with pressurized fresh air. The EGR loop was used in Paper 1 and Paper 3, whereas the EGR valve was sealed off in Paper 2 and Paper 4.

The DOC used in Paper 3 was a metallic catalyst (Pt:Pd), operating at the engine exhaust temperature of $215 \pm 6°C$. This custom-made aftertreatment unit was dimensioned to fit the one-cylinder heavy-duty engine, so that the exhaust residence time could be considered representative of the real engine operation.

4.1.2 Measurements, data collection and analysis

Data collection started after the engine coolant and oil temperature reached 85°C during the warm-up test runs. The in-cylinder pressure data were collected from the engine by sampling signals every 0.2 CAD and averaged from 300 engine cycles for every operating point under steady state conditions.

A water cooled Kistler piezoelectric pressure transducer measured the relative in-cylinder pressure. The cylinder pressure at the inlet bottom dead center (BDC) was considered equal to the intake manifold pressure when the absolute in-cylinder pressure was calculated for the heat release calculations. Also, the TDC offset between the CAD measured by the encoder signal and the calculated in-cylinder volume was compensated for by setting the peak of the motored in-cylinder pressure at a fixed location, as explained in [185].

The value of lambda (λ) was measured and monitored in real time by an ETAS LA4 meter. The fuel consumption was estimated from the slope of the fitted linear regression model of the fuel tank weight continuously measured by a Sartorius gravity scale.

The data post-processing procedure was based on the calculations of the rate of heat release (RoHR), in-cylinder volume, pressure and temperature, indicated mean effective pressure (IMEP) and efficiencies (combustion and gross indicated) described in Chapters 2, 4 and 5 of [186] and in [162]. The mixing period (MP) was calculated as the crank angle degrees between the end of injection (EOI) and start of combustion defined as CA5.

4.1.3 Fuels and lubricants

Fuels used in this work were Swedish fossil low-sulfur diesel MK1 (referred to as fossil diesel, or diesel), neat diesel-like renewable fuels, RME and HVO, neat light alcohols ethanol and methanol, as well as two mixed fuels B20 (20% by volume RME, 80% by volume MK1) and E85 (15% fossil gasoline, 85% ethanol). The properties of these fuels are given in Table 4.

Table 4. Fuel specifications.

	diesel	HVO	RME	methanol	ethanol	E85
RON	–	–	–	107–109	108–109	101–104
MON	–	–	–	92	89	–
CN	~53	>70	52	–	–	–
H/C	2	2.143	1.896	4	3	2.703
O/C	0.02	0	0.103	1	0.5	0.382
Q_{LHV} [MJ/kg]	43.15	44.1	37.3	19.9	26.7	29.62
(A/F)$_s$	14.5	14.9	12.37	6.47	9	9.85

In order to increase the lubricity of the alcohols used (methanol, ethanol and E85) and ensure flawless operation of the fuel delivery system, 200 ppm of Infineum R655 was added to the E85, and 300 ppm to methanol and ethanol. Its effect on the results was considered negligible [187]. This additive was not necessary when diesel fuels were used.

The lubrication oil in the engine in Paper 1 and Paper 2 was Statoil PowerWay GE40, a lubricant with low ash content used mainly for engines operated on biogas. In Paper 3 and Paper 4, the lubricant used was synthetic low-ash motor oil (Shell Mysella S3 N40). After the experiments in Paper 1 and Paper 2 were completed, samples of fuels, unused engine oil and used engine oil were sent to an external laboratory for analysis.

4.2 Emission measurements

4.2.1 Gaseous exhaust

In the first experimental rig, the engine-out gaseous emissions without an aftertreatment system were measured by a commercial AVL AMA i60 system, and in the second experimental rig by a Horiba emission system (MEXA-7500DEGR). Their principle of operation was same. The CO_2 concentration was measured both in the intake manifold and in the exhaust to provide the data for the calculation of

the EGR level. The dry CO and CO_2 were measured with an infrared detector (IRD), whereas the wet NO and NO_x ($NO+NO_2$) were measured using a chemiluminescence detector (CLD). The wet total hydrocarbons (THC) emissions were measured by a flame ionization detector (FID). The THC was summed as $C_aH_bO_c$ or $CH_{b/a}O_{c/a}$, and the CH_4 concentration was measured within it.

The flame ionization detectors in the emission analyses were not optimal for measurement of exhaust from oxygenated fuels, such as E85 in Paper 4, since they underestimated the THC concentration. The same was valid for methanol and ethanol in Paper 2, but these emissions were not presented in the paper. According to studies [188][189], the realistic THC values in E85 exhaust may be higher by 15–18% than the ones measured by FID. However, the suggested correction factors were not included in the results presented in this thesis nor in publications.

The EGR levels used in Paper 1 and Paper 3 were calculated as a ratio between measured concentrations of carbon dioxide in the intake and carbon dioxide in the exhaust, expressed as percentage, as shown in Equation (1).

$$EGR = \frac{CO_{2\,Inlet}}{CO_{2\,Exhaust}} \cdot 100\% \qquad (1)$$

The O_2 concentration in the exhaust was measured by a paramagnetic detector (PMD), and the intake O_2 concentration was calculated according to Equation (2).

$$O_{2\,Inlet} = EGR \cdot \left(O_{2\,Exhaust} - O_{2\,Ambient}\right) + O_{2\,Ambient}, \qquad (2)$$

where $O_{2\,Exhaust}$ is the oxygen concentration measured in the exhaust, and $O_{2\,Ambient}$ is the ambient oxygen concentration set to a constant value of 20.95%.

Exhaust gas analysis was performed by using equations presented in Chapter 4 of [186]. In Paper 1 and Paper 3, λ yields:

$$\lambda = \frac{1}{2\cdot\left(a+\frac{b}{4}-\frac{c}{2}\right)} \cdot \left[\frac{a}{a\cdot x_{THC}+x_{CO}+x_{CO_2}} \cdot \left(c \cdot x_{THC} + x_{H_2O} + 2x_{O_2} + x_{CO} + \right.\right.$$
$$\left.\left. 2x_{CO_2} + x_{NOx}\right) - c\right], \qquad (3)$$

where values a, b and c come from the fuel formula $C_aH_bO_c$, i.e. $a = 1$, $b = $ H/C and $c = $ O/C (see Table 4), and x represents a measured or calculated concentration of a gas species. Oxygen concentration measurements of the exhaust were not available in Paper 4, and values measured by the ETAS sensor were used instead.

The values of the gaseous emissions and soot mass concentrations were presented as indicated specific (IS) values, i.e. the amount of a pollutant per useful work, in Paper 1 , Paper 2 and Paper 4, and these IS emissions will be in the thesis text called

by the name of their constituents. In Paper 3, emission factors were used instead. They represent the amount of pollutant per energy content of the consumed fuel, as defined in [49]. Relative standard deviations based on the time-series of HC measurements used for calculation of emission factors were 5–10% for all fuels.

4.2.2   Particulate matter

Black carbon and organic fractions of PM in engine exhaust were analyzed, as well as metals found in PM.

4.2.2.1   *Mass concentration and size distribution*

An AVL micro-soot sensor (MSS) was used in Paper 1, Paper 2 and Paper 4 to continuously measure the equivalent black carbon (eBC) mass concentration of soot in the engine-out exhaust stream. Measurements are based on the photo-acoustic principle, as explained in [190]. Inside of the measurement cell, an amplitude modulated 808 nm light beam is absorbed by airborne particles. This makes the carrier gas expand and contract due to periodic heating and cooling, and in that way produce periodic pressure waves. The pressure waves are a measure of the particle absorptive properties (at 808 nm), and are gathered by sensitive microphones and translated into a soot mass concentration (eBC) by assuming a conversion factor from absorption to mass concentration. The BC part of the PM absorbs, while OA is essentially transparent at this wavelength, and therefore not measured. The MSS is able to measure with a sensitivity of 1 $\mu g/m^3$ in the range from 0.001 to 1000 mg/m^3.

A differential mobility spectrometer (DMS) Cambustion DMS500 was used in Paper 1 and Paper 2 to determine the particle size distribution (5 nm – 1000 nm) [191]. Measurements were sampled with a frequency of 1 Hz. At the sampling probe, a cyclone was used to dilute the exhaust gas at a ratio of 5:1. After two sages of dilution, the particles are charged by a unipolar corona charger. The charge they receive is proportional to their surface area and their size, and particles are separated according to electrical mobility while passing a strong radial electrical field. Larger particles with lower electrical mobility travel further along the column. This principle is also known as electrical mobility classification. After the particles get deposited on one of the 22 electrometer detectors, the measured electrical current signals are finally transferred into a number particle size distribution using the built-in diesel soot inversion matrix.

The AVL MSS and DMS500 sampled gas directly from the exhaust pipe.

4.2.2.2   *TEM*

The soot carbon nanostructure was analyzed in Paper 1 and Paper 2. After passing through a dilution system which was mounted perpendicularly to the exhaust pipe,

aerosol samples were collected from the exhaust gas onto thin lacy carbon coated copper grids using an electrostatic precipitator (nanometer aerosol sampler, TSI Inc.). These transmission electron microscopy (TEM) grids were analyzed in transmission electron microscopes. The dilution setups and microscopes, as well as analysis procedures, are described in detail in the respective papers.

4.2.2.3 Chemical composition

In order to determine the chemical composition of the emitted particles, three different techniques were used.

The first technique is aerosol mass spectrometry (AMS), an on-line technique that provides chemical characterization of the ensemble of sampled OA, without details on individual molecules or on particle-to-particle basis, but with the advantage of fast acquisition times, providing near real-time data. Additionally, it provides bulk properties of the complete organic fraction in the PM. For example, the elemental composition given as O:C and H:C ratios. The AMS and its quantification of OA are described in detail in [192] and the references therein. In brief, by means of an aerodynamic lens, AMS focuses aerosol particles directly from the dilution system into a narrow beam. The beam impacts a heated tungsten surface at 600°C, and the resulting vapors are ionized by means of electron impact, and then detected in a time of flight mass spectrometer.

The second method, the soot-particle aerosol mass spectrometry (SP-AMS), uses AMS for measurements of quantitative aerosol mass loadings from coating materials (e.g., organics, sulfates, nitrates, etc.) and it additionally measures the mass of the refractory carbon (rBC) cores (i.e. BC mass).

In paper 1, the total OA was analyzed using a SP-AMS [193]. The SP-AMS was run in single or dual vaporizer mode. The total OA signal intensity depends on the vaporization mode. In the single vaporizer mode, particles are flash vaporized, as in AMS. In the dual vaporizer mode, rBC containing particles are vaporized using an intracavity Nd:YAG laser (1064 nm). In order to derive OA mass concentrations, the dual vaporizer total OA signals were multiplied by a correction factor of 0.5 which was obtained from the linear regression analysis of a large number of total OA single mode and dual vaporizer mode ratios ($R^2 = 0.93$).

In Paper 3, the software SQUIRREL 1.62 and PIKA 1.22 were used for data analysis and recommended practice was followed with one exception. The standard procedure is to take a HEPA filtered background air sample without particles, by which the gas phase contribution to m/z 44 signal (CO_2^+) can be quantified. This was not done in our experiments, but instead the amount of CO_2^+ that should be subtracted was estimated from a $CO_2(g)$ monitor, assuming that the gas phase signal scales linearly with the measured sampling line mixing ratio in the range of 0–500 ppm.

Thirdly, in Paper 2, the TEM was equipped with a silicon drift detector (SDD) based energy dispersive x-ray analysis (EDX) system. EDX is an x-ray technique used to identify the elemental composition of materials. The data generated by EDX analysis consist of spectra showing peaks corresponding to the elements making up the true composition of the sample being analyzed.

4.2.3   Aging of emissions

In Paper 3, an oxidation flow reactor (OFR) was used to simulate secondary aerosol formation and changes in OA composition upon atmospheric aging [194]. The potential aerosol mass (PAM) reactor uses UV light to initiate oxidative gas phase chemistry and simulates the equivalent of several days in the atmosphere during a few minutes' residence time in the OFR. The detailed procedures are reported in [49] and are only briefly repeated here. The PAM-reactor consists of a 13 liter steel chamber containing two Hg lamps with peak intensities at 185 and 254 nm, however only one of the lamps was used and operated at a reduced intensity for all experiments. The flow rate through the PAM was controlled to 5–7 lpm, resulting in an average residence time of 113–160 s in the chamber. The incoming water vapor concentration was 0.37 ± 0.02 mol/m^3. CO (40 ppm) was added to the flow to allow calculation of the OH exposure in each experiment. The cumulative OH exposure was calculated from the reaction rate constant of CO and OH, and the CO concentrations. Due to variations in flow rate and OH suppression, the OH exposure varied somewhat between experiments. The OH exposure (molecules cm^{-3} s) corresponded to 4.8 ± 2.6 days if assuming an average OH concentration of 1.5×10^6 molecules cm^{-3}.

4.3 Planning experiments and engine operating conditions

Before conducting experiments, initial pre-studies were performed in order to determine the limits of different engine control parameters. These experiments were designed to give a fundamental understanding of differences between the fuels, and their effect on the engine performance and emissions. In Paper 1 and Paper 4, the regulated emissions were compared to Euro VI emission limits, whereas the scope of Paper 2 and Paper 3 did not include comparison of engine emissions to the legislations.

An overview of the operating conditions in the experiments is given in Table 5. Heavy-duty engines operating over low load duty cycles are typical for urban environments that require large quantities of goods deliveries and services for commercial and domestic use such as refuse pickup. For this particular engine, a

load of 6 bar gross indicated mean effective pressure (IMEP$_G$) is considered low load, the IMEP$_G$ of 8 bar is mid-to-low load, and the IMEP$_G$ of 10 bar is mid load.

In Paper 1, the intake oxygen concentration was scanned by changing the EGR level. It resulted in λ changing within a range from 2 for the highest intake oxygen concentration (O$_{2in}$), to 1 for the lowest O$_{2in}$. In Paper 2, two engine loads were tested, where λ was 3 for the lower load and 1.9 for the higher load. All experiments in Paper 3 were performed under unchanged operating conditions. In Paper 4, a design of experiment (DOE), Box-Behnken design (BBD) in particular, was applied in order to, with a limited number of measurement points, collect the data that can characterize a wide field of operation with E85. The control parameters, fuel injection pressure (P$_{rail}$), air-fuel ratio expressed as λ, and combustion phasing measured after top dead center (ATDC) as the crank angle at which 50% of the charge has been consumed (CA50), were varied at three different levels. In order to study the effects of these engine control parameters on the engine behaviour, five multiple linear regression (LR) models of engine gross indicated efficiency (GIE), IS THC, CO, NOx and soot were built.

Gross indicated efficiency is a measure of the total work provided by the combustion of the fuel when combustion loss, heat transfer loss and exhaust loss have been accounted for. Since the experimental engine is modified to operate on one of six cylinders, it is not possible to know the friction losses in order to calculate brake efficiency. Moreover, the pumping loop of the engine was not provided by the manufacturer, so net indicated efficiency could not be estimated. Therefore, the efficiency in this thesis (Paper 4) is presented as GIE.

Table 5. Engine operating conditions in the experiments.

	IMEP$_G$ [bar]	T$_{in}$ [°C]	O$_{2in}$ [%]	P$_{rail}$ [bar]	CA50 [CAD ATDC]	λ	fuels
Paper 1	6	100	~8, 11.5, 13.5, 15, 20.95	1200	5	0.8 – 2	diesel, RME
Paper 2	6, 10	30 (diesel), 110	20.95	1200	5	3, 1.9	diesel, methanol, ethanol
Paper 3	6	26–28	18	1200	5	2 – 2.5	diesel, RME, HVO
Paper 4	8	120	20.95	800, 1000, 1200	6, 8, 10	1.25, 2.3, 3	E85

5 Results and discussion

This chapter discusses the results of the studies presented in the four papers on which this thesis is based. The results are divided into two main parts; the first part reports on the combustion of diesel-like fuels (based on Paper 1 and Paper 3), whereas the combustion of the light alcohols is addressed in the second part (based on Paper 2 and Paper 4). The focus of the first part lies on analysis of particulate matter, both soot and organic aerosol, with a reflection on the effect that renewable diesel-like fuels have on the emissions from a compression ignition engine under low load operation. The second part highlights the benefits of using non-sooting alcohols in a compression ignition engine, and examines the structure and composition of the emitted nanoparticles. The third part of the results is discussing structure of soot in the engine exhaust analyzed by means of TEM imaging (from Paper 1 and Paper 2). In the final part of the results, possible origins of particles are summarized from findings in Paper 1, Paper 2, and Paper 3.

5.1 Diesel-like fuels

5.1.1   Combustion

In order to isolate the effect of replacing fossil diesel fuel with renewable diesel-like fuels on the emissions, the experiments were designed in such a way to achieve comparable low temperature combustion conditions for the three fuels with low EGR levels in the first experiments (Paper 3), by keeping the same ignition delay period (the CAD between the start of injection and start of ignition) and similar mixing period, and therefore removing the influence of different cetane number of the fuels. The same adjustments were made for the conventional diesel combustion with no EGR shown in Figure 9, as well as for the other engine settings in Paper 1. The rate of heat release and in-cylinder pressure traces within a relevant window of crank angles are shown in Figure 8 for diesel, HVO and RME, and in Figure 9 for diesel, B20 and RME.
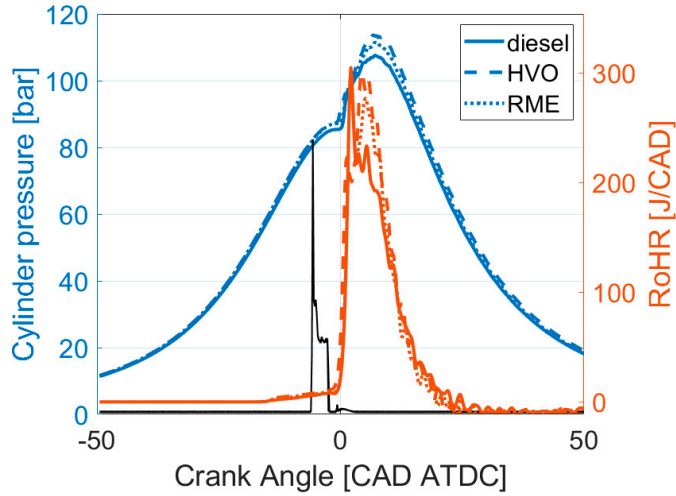
Figure 8. RoHR, in-cylinder pressure, and injector current for diesel, HVO and RME.
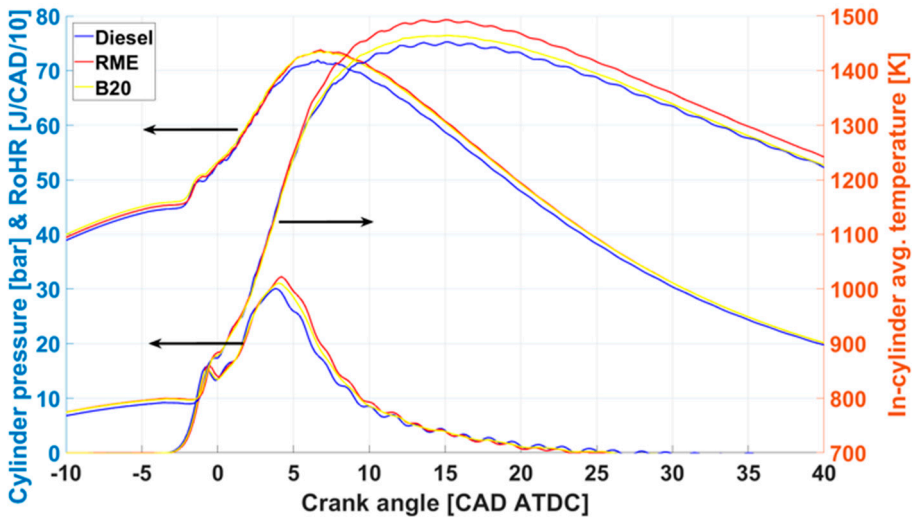
Figure 9. RoHR, in-cylinder pressure, and in-cylinder average temperature for diesel, RME and B20 at ~21% O_{2in}.

The combustion characteristics of renewable diesel-like fuels are close enough to fossil diesel that these fuels can be used almost interchangeably without any adjustments in the engine. The fuel analysis of RME showed 10.6% mass oxygen content compared to that of diesel at 0.2%. As the combustion duration is not significantly different between the fuels, the difference in soot is not down to differences in post-combustion soot oxidation.

5.1.2   Emissions

5.1.2.1   *Gaseous emissions*

In the experiments from Paper 1, the engine operation conditions were not optimized to suppress any specific emissions. Instead, the goal was to compare how utilizing different EGR levels affects regulated and unregulated emissions. This resulted in very high NOx emissions for the operation point without EGR, highest for RME, and followed by B20 and diesel (20% lower than RME). Both the additional oxygen available and the high degree of unsaturation of fatty acids in RME fuel may have contributed to high NOx levels, as discussed in literature [195][196]. At the base operating point without EGR, RME was burning at a higher combustion temperature than diesel, further promoting NOx formation (Figure 9). This may be due to a stronger effect of lower stoichiometric A/F ratio, and in turn lower local cylinder gas entrainment which increases local combustion temperatures, compared to the effect of lower fuel energy content resulting in a higher ratio of stoichiometric fuel mass and released fuel energy, which entails lower local combustion temperatures [197].
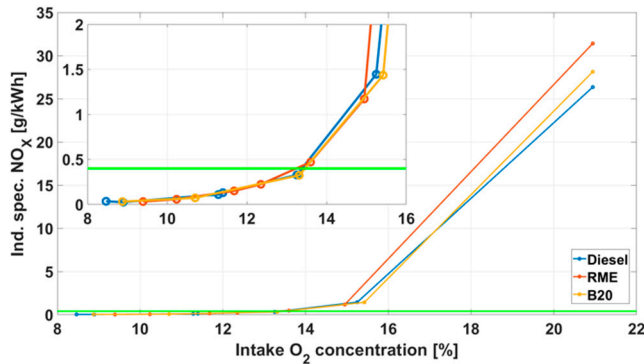
Figure 10. Indicated specific NOx emissions for different O_{2in} concentration for diesel, RME and B20.
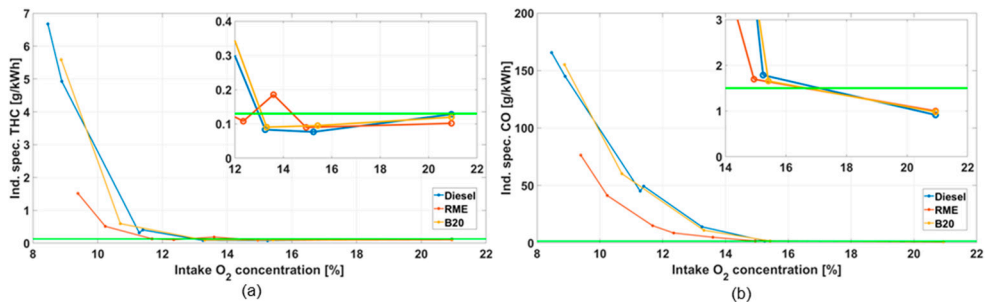
Figure 11. Indicated specific (a) THC and (b) CO emissions for different O_{2in} concentration for diesel, RME and B20.

The THC and CO emission levels were increasing rapidly with decreasing of the oxygen available for combustion below 13% and 15% for all three fuels, as shown in Figure 11. The values of these emissions were almost at the same low levels for higher O_{2in} concentrations for all fuels, whereas RME had favourable emissions compared to diesel and B20 for lower intake oxygen, due to more abundant fuel-borne oxygen. The horizontal green lines in Figure 10 and Figure 11 represent the Euro VI emission limits.

5.1.2.2 Particulate matter

The soot (eBC) mass concentrations for diesel, RME and B20 were strongly affected by EGR, and their values over the range of O_{2in} levels are presented in Figure 12.
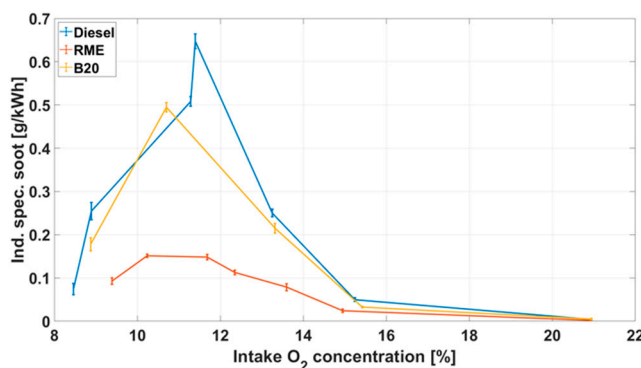
Figure 12. Indicated specific soot (eBC) mass concentration for different O_{2in} concentration for diesel, RME and B20.

A certain improvement in the soot mass concentration is already seen for B20 compared to diesel, but RME emits considerably lower levels of soot over the whole range of O_{2in} concentration, as an earlier study also reports [198].With low or no EGR, FAME fuels decrease BC emissions by about a factor of 2 according to [34], which matches our RME results at intake O_{2in} of ~21% and ~15%. The reduction factor increased to 3–4 at high EGR levels. This provides the possibility to use higher levels of EGR (lower O_{2in} concentration in Figure 12) with RME if the combustion is to result in the same soot levels like those produced when combusting diesel. The NOx-soot trade-off was less pronounced and staying in the region of low NOx, as well as CO and THC emissions, was possible.

To be precise, the intake oxygen level of ~15% that corresponds to EGR of ~37–39%, is close to a typical EGR level used in a modern HD CI engine. NOx values at O_{2in} of ~13.5% (~44% EGR) for all three fuels werere only 23% to 40% of the NOx values at ~15% O_2. The indicated specific soot value of RME at O_{2in} of ~13.5% was below 0.1 g/kWh.
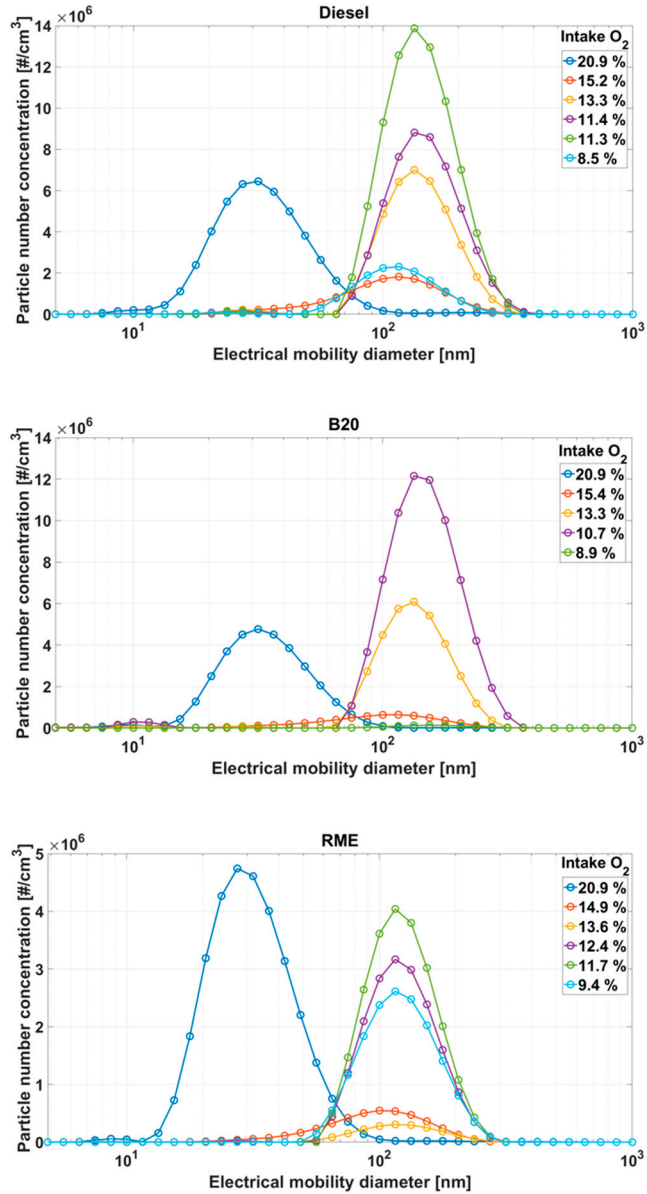
Figure 13. Number weighted particle size distributions for different O_{2in} concentration for diesel, RME and B20, top: diesel, middle: B20, and bottom: RME.

Figure 13 presents the electrical mobility particle size distribution for the different O_{2in} concentrations for the three fuels, note the different scale for the particle number concentration for RME. Without EGR, a nucleation mode dominated the emissions (20–30 nm), while for the remaining cases an accumulation mode at larger particle

sizes dominated the number emissions (Figure 13). The particle count median diameter (CMD) is a parameter that describes the modes and is equal to the diameter with highest concentration if the distribution is lognormal. Diesel had the highest CMD values within the whole O_{2in} span (with an exception of the lowest O_{2in} level), followed by B20 and RME, which agrees with the results available in literature, e.g. [199]. The values of accumulation CMD for the lower O_{2in} values lay in the range from 125 to 160 nm, whereas at the O_{2in} of ~21%, the mean diameter was lower as the accumulation and nucleation mode strongly overlapped.

Since the nucleation mode was dominant only when operating without EGR, the indicated specific total TPNC (including total particle number count for both nucleation and accumulation modes) trends followed the soot mass concentration measurements, see Figure 12, in the whole O_{2in} range apart from the starting point at ~21%. Note that the nucleation mode measured here includes particles of size 5 nm and above, and may include some liquid nucleation mode PM, whereas Euro VI regulates only solid particles larger than 23 nm.

The intake oxygen levels were comparable among the three fuels at four levels:

- ~11.5%: total TPNC of RME was lower than half the value for diesel;

- ~13.5%: total TPNC of RME was significantly lower, in particular it was only 6% of total TPNC of B20 and 5% of that of diesel;

- ~15%: the advantage of RME was not as pronounced as in the previous point, since total TPNC of RME was similar to the one of B20, but more than three times lower than that of diesel;

- ~21%: when EGR was not utilized RME and B20 had similar total TPNC, while that of diesel was 50% higher.

There was a clear advantage of using RME with EGR rates as high as 44% in terms of indicated specific TPNC under the studied engine operating conditions. Even B20, a low biodiesel content blend, already gave visible results in soot mass reduction.

5.1.2.3   Organic aerosol

Based on the experiments in Paper 1, Figure 14 shows the ratio of total (particle phase) OA measured with SP-AMS, and eBC measured with MSS for different O_{2in} concentrations for diesel, RME and B20. At O_{2in} of ~21%, the organic mass fraction of the PM emissions was dominant, being three times higher than the eBC mass fraction for diesel and two times higher for B20 and RME. Since the combustion temperature of diesel at ~21% intake oxygen concentration was lower than that of RME, as shown in Figure 9, this difference between RME and diesel might be due to the incomplete combustion of lubrication oil that was consequently emitted in the exhaust. Paper 2, Paper 3 and other previous studies, see [138][139][142][149],

report that the mass spectra of diesel aerosol components are dominated by lubrication oil spectral structures. However, most of the lubrication oil PM comes from slip that escapes combustion at low loads [20][200].

When values in Figure 12 and Figure 14 were compared, it could be seen that in general OA emissions are 2–3 times lower for RME than for diesel. Diesel, RME and B20 had very low OA to eBC ratio for higher EGR levels. For oxygen concentrations lower than ~13.5%, the ratio for RME was slightly higher than for B20 and diesel due to the lower soot emissions in that area. Finally, at the highest EGR level with 8.5% O_{2in} concentration, the ratio for diesel again rose and reached the value of one. At this point, a low amount of eBC was emitted, so the ratio of one showed low OA emissions. It is also possible that the soot did not have time to mature to eBC, i.e. soot precursors such as PAHs and brown immature soot were emitted. Soot formation slowed down at very high EGR [32]. Additionally, the combustion efficiency was very bad there as the engine was below stoichiometric conditions ($\lambda = 0.85$) and emitted unburned fuel. The reason for studying this extreme condition was to see how the emissions would look like in an event of failure of an engine part or system that would cause high levels of exhaust gas recirculated to the engine intake.
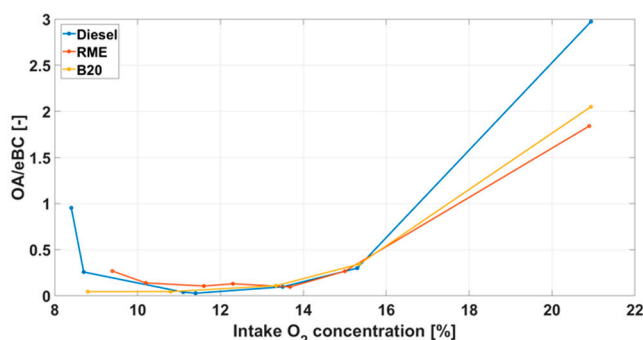
Figure 14. OA/eBC for for different O_{2in} concentration for diesel, RME and B20.

In Paper 3, the OA mass emissions were measured by AMS. Figure 15(a) shows that emission factors of HC (gas phase) and OA (PM fraction of organics) for HVO were slightly lower than those of diesel, around 20% and 30% respectively. At the same time, emission factors were around three times lower for RME compared to diesel, for both HC and OA, which is in line with the aforementioned results from Paper 1.

Secondary organic aerosol from traffic can be a major contributor to long range transported PM$_{2.5}$ in the atmosphere. In order to estimate atmospheric aging of the organic emissions over a period of several days, which may cause changes in the OA composition, the SOA formation was simulated in an oxidation flow reactor

[194]. It can be seen in Figure 15(b) that aged OA emission factors were highest for diesel, about 2 times lower for HVO and about 8 times lower for RME. Similar to fresh OA, RME formed considerably less aged OA than the other fuels. The OA enhancement was very high measured at engine out (EO), it gave almost 20 times higher aged OA mass compared to fresh emissions of diesel, and 6 times higher for RME, see Figure 15(b). The OA mass enhancement estimation is probably on the higher side, since the nucleation mode particles smaller than ~40 nm in fresh OA without DOC are invisible to AMS, whereas they get detected after aging when they grow considerably due to condensation [49].

(a)   (b)
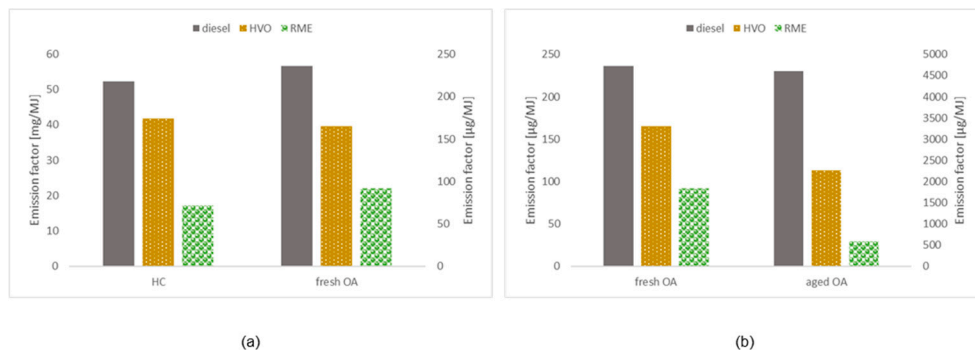
Figure 15. The emission factors of (a) gaseous HC (left axis) and the fresh OA fraction in PM (right axis), and (b) the fresh OA fraction in PM (left axis) and aged OA (right axis), for diesel, HVO and RME measured engine-out. Note different scales on the left and right axes.
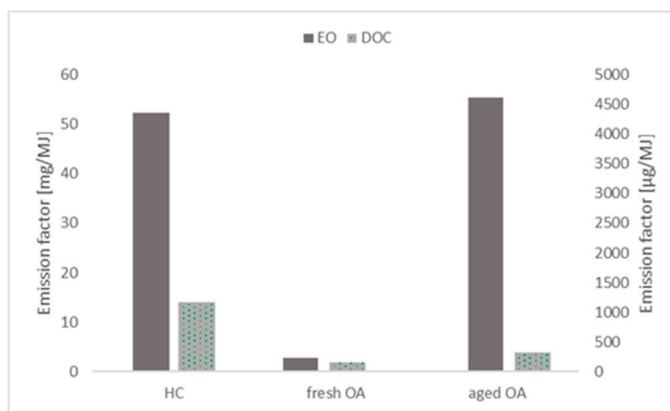
Figure 16. The emission factors of gaseous HC (left axis), the fresh OA fraction in PM (right axis) and aged OA (right axis) for diesel measured engine-out and after DOC. Note different scales on the left and right axes.

When the values of hydrocarbon precursors in Figure 15(a) are compared to aged OA values in Figure 15(b), it can be seen that for diesel ~9% of the gas phase HC was converted to particle phase OA in the atmosphere. These numbers were lower

for the two renewable fuels (near 5% for HVO and 3% for RME), which might be due to differences in the chemical composition of the gas phase HC. Namely diesel aromatic compounds and medium and long chain aliphatic compounds have a high SOA yield, while the SOA-yield of short chain aliphatics is much lower [201].

Figure 16 compares HC, fresh OA and aged OA for EO and after a DOC, only for diesel emissions. The DOC introduces a strong reduction in all three cases. The strongest reduction is achieved for aged OA by a factor of more than 10. When an engine operates at low load, exhaust temperatures tend to be lower, which can result in the DOC being less effective. In this experiment, however, the DOC was operated at around 215°C [49], which was not far from an appropriate temperature for high HC reduction. Further analysis of the effect of the DOC on fresh and aged emissions from HVO combustion will be presented at the end of Chapter 5.4.

5.2 Light alcohols

5.2.1 Engine performance

In order to characterize the engine performance and emissions, without exposing the engine to the extreme settings of the control parameters, 13 engine operating points to be tested were chosen according to a Box-Behnken design of experiments. The most important engine control parameters, P_{rail}, λ and CA50, were varied at three levels each, low, medium and high, shown in Table 6. With a limited number of measurement points, BBD helped to collect the data that could characterize a wide field of DICI operation with E85 fuel. A detailed description of the method is given in Paper 4.

Table 6. Physical values of the BBD factors.

P_{rail} [bar]	λ	CA50 [CAD ATDC]
800	1.25	6
1000	2.3	8
1200	3	10

As a support in analyzing the experimental results, in order to mathematically describe the effects of the control parameters on the engine behaviour, as well as to determine interactions between them which otherwise might not be obvious, linear regressions models were made. The five built models represented GIE, and IS THC, CO, NOx and soot emissions. The models had a high quality fit to the measured data.
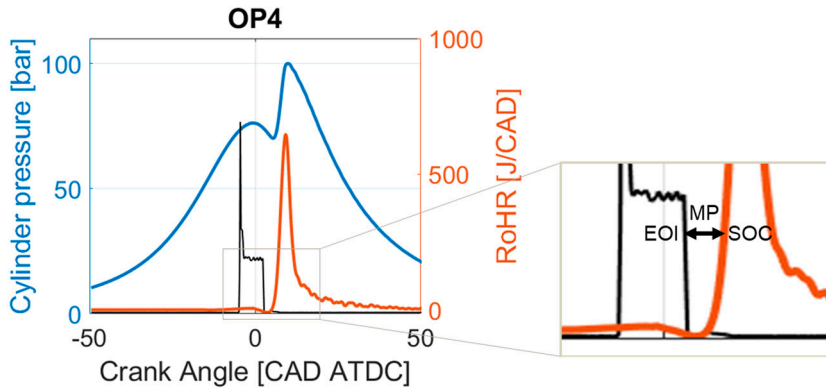
Figure 17. RoHR, in-cylinder pressure, and injector current for OP4 with E85; the zoom is on the mixing period. For the OP nomenclature, see Paper 4.

An example of the RoHR, in-cylinder pressure and injector current within a relevant window of crank angles for the engine operating point (OP) number 4 (P_{rail} = 800 bar, the low setting; λ = 3, the high setting, and CA50 = 8 CAD ATDC, the medium value) is shown in Figure 17. In order to indicate the start of injection (SOI) and EOI, the injector current was represented with a black line. The relevant window around TDC is zoomed in and shown on the right-hand side of the figure. The end of injection was clearly separated from the start of combustion resulting in a positive mixing period. This indicated that the combustion mode was LTC, PPC in particular, which was the case for all 13 studied operating points. The combustion durations were very short, which was one of the factors contributing to high efficiency.
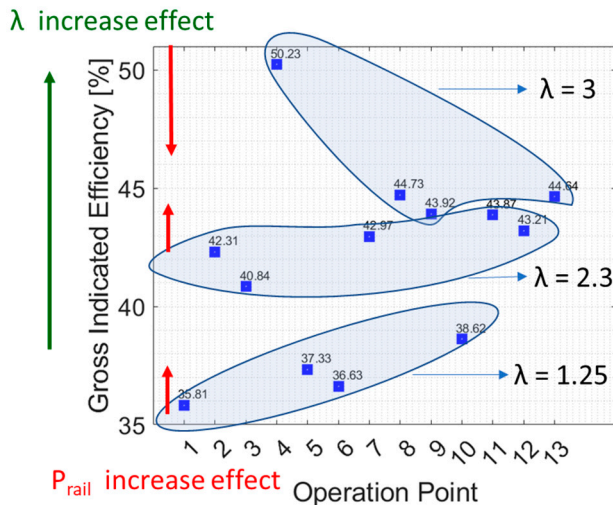
Figure 18. Gross indicated efficiency for the 13 OPs with E85. For the OP nomenclature, see Paper 4.

The majority of operating points lay in a GIE range right below 45%, see Figure 18. The group of OPs with λ at 1.25 with lowest GIE (OPs: 1, 5, 6 and 10) had the highest maximum average in-cylinder temperatures resulting in higher heat losses, but low THC emissions due to high temperatures, see Figure 19. Higher CO emissions (also in Figure 19) resulted in their combustion efficiency being slightly lower than of the other OPs.

The next group of OPs with λ at 2.3 (OPs: 2, 3, 7, 11 and 12) had medium values of GIE. The maximal in-cylinder temperature of OP4 was similar to those of OP2 and OP3, and it was reached at similar CAD, but the average in-cylinder temperature dropped faster for OP4 due to its shorter burn duration than for OP2 and OP3.

The group with highest GIE values contained operating points with λ at 3 (OPs: 4, 8, 9 and 13), which showed a clear effect of leaner combustion (see the green arrow in Figure 18). The effect of increasing P_{rail} (see red arrows in Figure 18) was positive for GIE at low and middle lambda setting, but when the mixture was already diluted to λ of 3, additionally increasing injection pressure possibly caused overleaning and reduced GIE.

The OP4, with the highest achieved GIE of 50.23%, was a candidate for the most favourable operation condition within the range tested in Paper 4. The reason for the high GIE might be that λ at 3 was better for thermodynamic efficiency, and that CA50 at the middle setting (8 CAD ATDC) was nearest to the optimal setting. That, in combination with the low P_{rail} of 800 bar, gave the operation conditions of this engine configuration that could be a starting point for a further investigation, due to a big step up in GIE compared to the other OPs.

5.2.2 Emissions

The trends of emissions were compared to the stationary Euro VI emission standards for HD vehicles, as well as to emission levels from literature and with diesel fuel results from Paper 1. In Figure 19 and Figure 20, the respective Euro VI limits are given in solid black line for CO, THC, NOx and soot, and in Figure 22, the green line represents the 23 nm particle measurement limit.

5.2.2.1 *CO and THC*

The results from LR models of THC and CO indicated that the level of these pollutants in the exhaust depended strongly on λ. A dependency between THC and CO which was close to linear, can be seen in Figure 19. The slope got less steep as λ increased, its effect marked with the green arrow, resulting in lower CO but higher THC emissions. Contrary to GIE, increasing P_{rail} had a positive effect on the group of OPs with λ at 3, see the red arrow in Figure 19. This was the case also for λ = 2.3, whereas both CO and THC levels were increased for higher rail pressure at λ of 1.25.
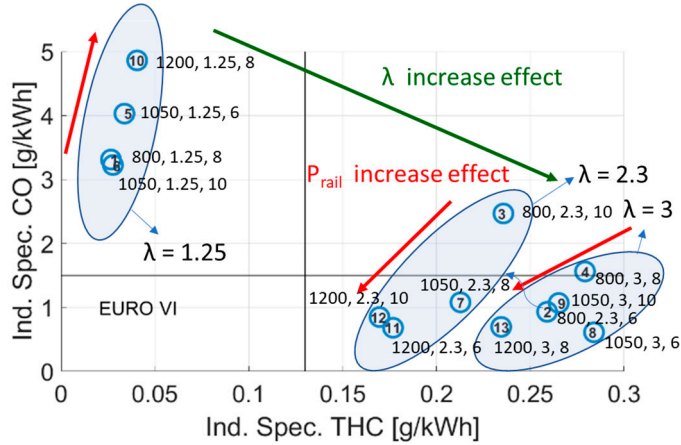
Figure 19. IS CO versus IS THC for the 13 OPs with E85. The OPs are marked with Prail, λ, CA50.

Operating conditions similar to OP11 studied in Paper 1, showed 25% lower THC emissions with diesel fuel, see Figure 11(a), compared to E85 in this study. Since the injectors used here were not targeted for the combination of E85 fuel in the existing engine, a different injector design would be a possible degree of freedom for lowering THC emissions. In general, it was expected that THC emissions would be higher due to higher latent heat of vaporization of ethanol compared to diesel.

Figure 19 shows that CO emissions were lower than the EURO VI standard, except for the OPs with low λ settings. More air available for the combustion provided the conditions for complete oxidation to CO_2. One exception to this was OP3 (see Figure 19), where λ was at the medium level: the CO emission was slightly increased, possibly due to the retarded combustion, leaving less time for oxidation after combustion.

5.2.2.2 NOx and soot

The formation rate of NOx has exponential dependency on combustion temperature, as explained in [162]. In attempt to mimic this non-linearity, the linear regression model of NOx emissions included quadratic terms of P_{rail} and CA50.

Even soot formation and oxidation are non-linear processes. In this study, a LR model with control parameters: λ, showing the availability of oxygen and directly affecting the rate of soot oxidation, P_{rail}, indicating the mixing rate, and CA50, a measure of the time available for oxidation before opening of the exhaust port, was able to represent non-linearity of soot emissions, similarly to a previously described model in [202].

The emission measurements presented in Figure 20(a) show that the high λ value, with more oxygen available for the combustion, resulted in higher NOx emissions.

OP4 was the only exception to this, since the NOx level there was comparable to the OPs with the low λ values. The peak cylinder temperatures with leaner mixtures were considerably lower than for the OPs with lower λ values, still their NOx emissions were high. This difference may be due to higher latent heat of vaporization of ethanol compared to diesel, and its cooling effect which decreased NOx formation when the mixture was richer. At the higher λ settings, soot emissions were low, since more air was available for the oxidation. In order to see this, a part of Figure 20(a) is zoomed in and shown in Figure 20(b).
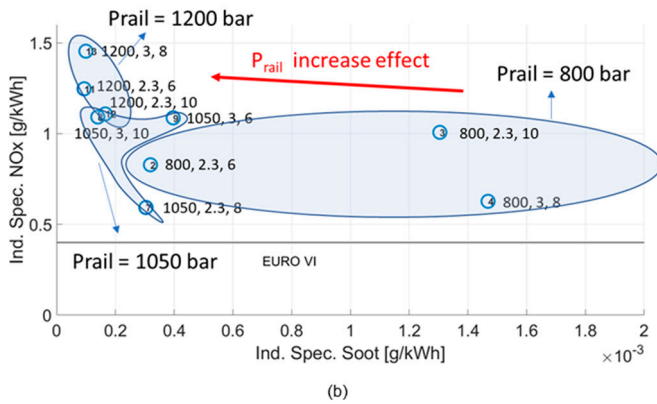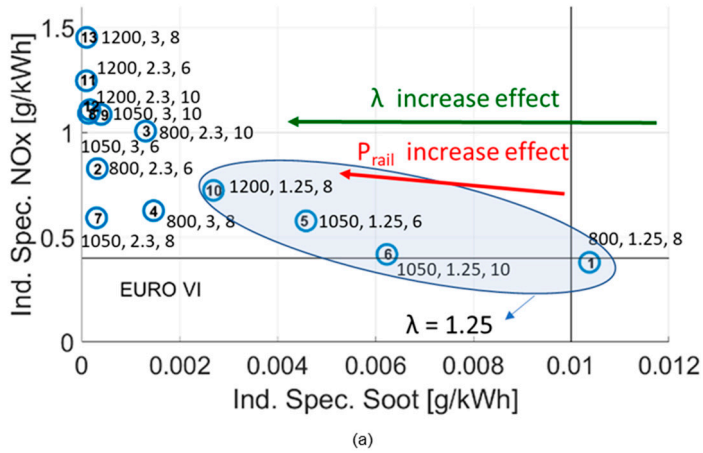
Figure 20. (a) IS NOx versus IS soot for the 13 OPs with E85; (b) plot zoom-in on low soot values. The OPs are marked with Prail, λ, CA50.

A higher P_{rail} increased the air entrainment and promoted fuel mixing rate by better fuel atomization and penetration, avoiding local rich zones, which resulted in lower soot levels. The combustion was, however, faster with shorter burn durations, and

higher peak in-cylinder temperatures, resulting in higher NOx emissions. The P_{rail} increase effect is marked by a red arrow in Figure 20, both (a) and (b).

Earlier combustion in combination with the P_{rail} increase gave higher increase in NOx emissions than later combustion when P_{rail} increased. Simultaneously, it allowed for longer time available for soot oxidation, reducing the soot levels.

Due to the PPC-type combustion of E85, where most of the combustion takes place in the premixed mode, NOx emissions were significantly lower relative to CDC observed in Paper 1. Still, the NOx levels were higher than the Euro VI legislation, and a reduction would be possible with EGR [59]. Soot levels were, however, under the Euro VI regulated levels, except for one OP.

Even a direct comparison of emissions from alcohols combustion to diesel emissions in Paper 2 confirmed that methanol and ethanol emit three to four times lower amounts of soot, see Figure 21. An earlier study [203] showed that the difference in exhaust soot mass concentration between diesel and the alcohols became more prominent when the engine was operated at conditions which would reduce soot oxidation, i.e. late cycle soot removal, for example high EGR levels, at an increased intake temperature and a low injection pressure. Soot mass concentrations never exceeded the Euro VI limit when running this engine using alcohols, while the values for gasoline PPC with EGR were 200 times higher [203]. The increase in soot emissions with increasing load for diesel was due to the reduced λ when running at higher loads.
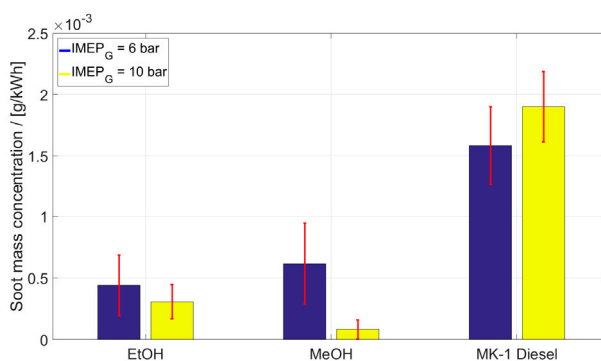

Figure 21. IS soot mass concentration for ethanol, methanol and diesel, for the two engine loads.

Both in Paper 4 and Paper 2, the average soot values were calculated from all 300 and 200 engine cycles, respectively. COVs of the measurements from MSS in operating points with lowest soot levels are over 20%, even though the sensitivity of MSS is such that it should be able to catch these low soot levels. Therefore, it can be argued that measured soot levels from alcohols combustion in these studies do not fall under measurement or experimental uncertainty, but that the actual soot

levels in certain OPs have high cycle-to-cycle variations. High COV values for cycle-resolved soot measurements are common, which is explained in detail in [204]. This difficulty to study soot mass concentrations for low-sooting fuels by the standard MSS techniques calls for new and more precise measurement sensors in future when the legislations get more stringent.

Particle number concentrations as a function of size distribution for low load (a) and for mid load (b) are shown in Figure 22. Methanol emitted the highest number concentration, followed by ethanol and diesel. Since the size distribution is dominated by nucleation mode particles both at low and mid load, the total particle number was not correlated to the soot mass concentrations, for the reasons explained in the introduction of this thesis.
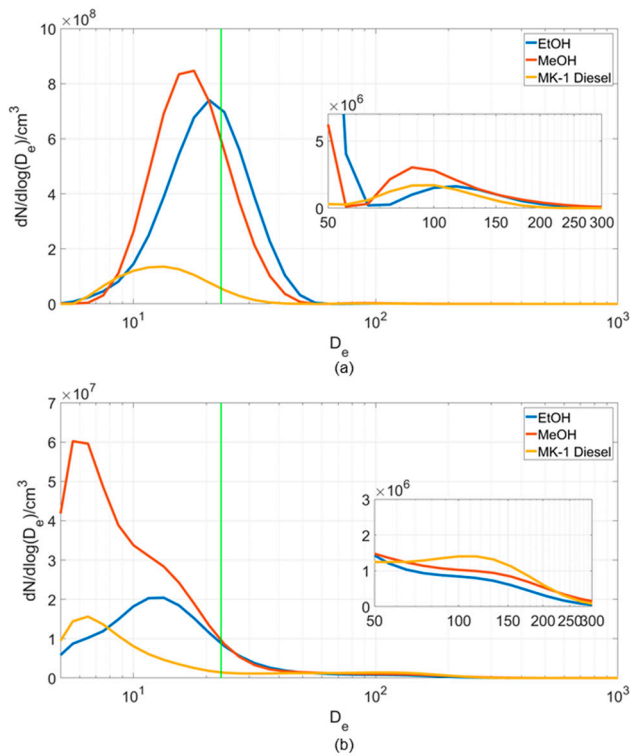
Figure 22. Number weighted particle size distributions for ethanol, methanol and diesel, at (a) IMEP$_G$ = 6 bar, (b) IMEP$_G$ = 10 bar.

At mid load, the nucleation mode CMD was reduced for all three fuels, compared to the low load. The reduction was highest for methanol at ~56%. This is visible in Figure 22, where the peak of the nucleation mode shifts to smaller particle sizes for higher load.

There was a slight increase in the accumulation mode region for diesel in relation to the alcohols at mid load compared to low load. Diesel emissions had larger agglomerates of soot in the accumulation mode, since the similar number count like for alcohols gave much higher mass concentrations. A decrease in the number concentration in the nucleation mode was observed when the nucleation mode particles rapidly coagulated with larger soot agglomerates at mid load. It could also be that when a larger soot surface area was available, the condensation of the lubrication oil and other OA happened to a larger extent on the soot. This means that less liquid nucleation mode particles may have formed as the required supersaturation for nucleation was not reached [49].

For the studied range of engine operation in Paper 4, Figure 20 shows that the NOx–soot trade-off could be better handled in combustion with E85 fuel due to its very low soot values and lower NOx values compared to similar low load conditions with diesel-like fuels previously studied in Paper 1. Even though NOx emissions were not analyzed in the experiments in Paper 2, the emitted soot levels from methanol were so low that the NOx–soot trade-off was non-existent even there. This opens a new possibility of supressing NOx emissions without fear of increasing soot emissions as a side effect.

Another interesting message from this chapter is that it may be possible to use a pump fuel E85 in legacy DICI engines with some modifications, and in that way reduce emissions and climate impact while continuing to use the engine throughout its lifetime.

5.3 TEM imaging

As presented in Paper 2, both soot agglomerates and spherical nanoparticles in the size range of 5 – 50 nm, consisting of one or more cores (see Figure 23), were seen in TEM images of particles from methanol and ethanol. Since a TEM image is a two-dimensional projection of a three-dimensional object, the cores of nanoparticles being brighter in images was an indication that they were either hollow, liquid, or consisting of elements lighter than the surrounding shells.

In the soot agglomerates, which in the particle size distribution fell under the accumulation mode as shown in Figure 22, nanoparticles were incorporated in the carbon structure. Therefore, the particles larger than 50 nm emitted from alcohol combustion could either be with or without the aforementioned lighter cores.

(a) ethanol detail   (b) ethanol overview   (c) diesel overview
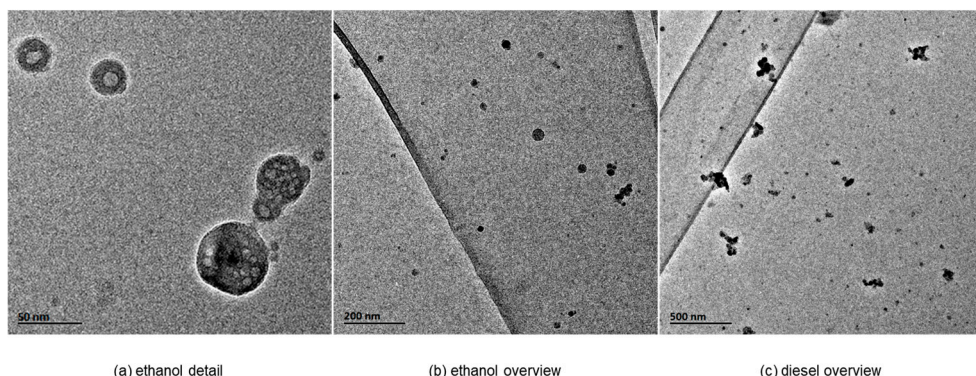
Figure 23. (a) Spherical nanoparticles with lighter cores emitted from ethanol (scale 50 nm), and overview TEM images of soot nanostructure for (b) ethanol (scale 200 nm), and (c) diesel (scale 500 nm).

Visibly different from the alcohol ones, particles collected on TEM grids originating from diesel combustion contained more soot agglomerates. This was confirmed in the next comparison between different diesel-like fuels presented in Paper 1 (see Figure 24). A few large clusters consisting of metallic nanoparticles were also observed in the diesel sample. This was not seen in methanol nor in ethanol.

Figure 24 shows the overview TEM images of soot agglomerates originating from combustion of (a) RME, (b) B20, and (c) diesel, at O_{2in} concentration of ~15%. When the two cases of different inlet oxygen concentrations (~15% and ~21%) were compared for each fuel, the overall appearance of their form, shape and density did not have any clear differences. The results were conclusive only for RME, indicating that at lower O_{2in} soot had higher reactivity, but at the same time layers within soot were less accessible for oxidation.

(a) RME   (b) B20   (c) diesel
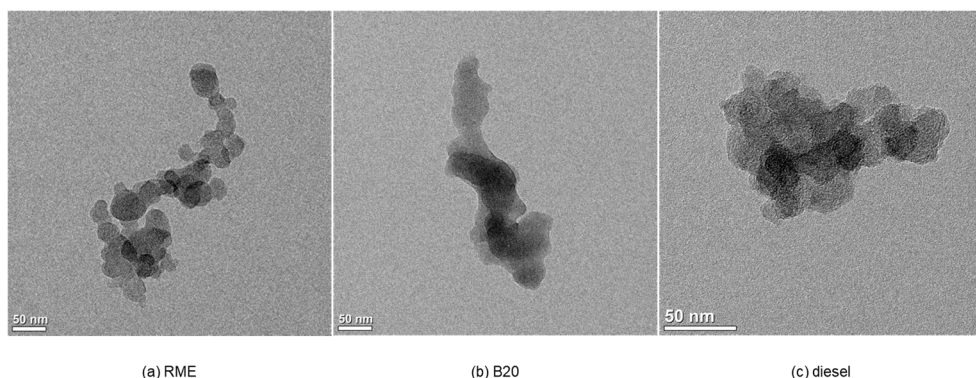
Figure 24. Overwiew TEM images (scale 50 nm) of soot nanostructure for the three fuels at similar O_{2in} concentration levels: (a) RME at 14.9%, (b) B20 at 15.4%, and (c) diesel at 15.2%.

The difference between the different types of fuel was more pronounced. Diesel and RME samples showed branched agglomerates composed of several tens to hundreds of primary particles between 20 nm and 30 nm in diameter. The samples collected from B20 also contained agglomerates of similar shape and size, however their structure was close to amorphous. The studied primary particles, however, seemed to be "melted" together and individual particles were not possible to distinguish (necking). Necking of primary particles is an element of soot morphology which should be considered when, for example, estimating the radiative properties of soot aggregates [205].

In addition to the regular soot particles, diesel samples contained some fly ashes, which were not present in RME soot samples. Fly ashes are usually seen as perfectly round-shaped spheres, slightly bigger than the single soot particles, sometimes even up to a micron in size. They are thought to originate from the burned engine lubrication oil droplets, as explained in [206].

5.4 Origin of particulate matter

Fuel and engine lubricant analyses were done in Paper 1 and Paper 2. Results from the analysis of the unused lubricant showed that minerals zinc (Zn), calcium (Ca), sulfur (S) and phosphorus (P) were the most abundant additives. The engine lubricant analysis in Paper 1 showed that iron (Fe) concentration of the used oil (6 weight ppm) was significantly higher than that of the new oil (1 weight ppm). If engine wear or corrosion particles would be seen on TEM grids, they would be separate particles not bound to any carbonaceous PM [206]. In this engine, the engine wear metals might have been collected by the lubricant instead of being emitted in the exhaust. The absence of Fe on TEM grids was confirmed by the EDX analysis in Paper 2.

The literature also reports that there is significantly less PM originating from engine wear than PM originating from the engine lubrication oil [206]. Soot (accumulation mode) acts as an efficient sink on which the nucleation mode particles can coagulate. In the absence of a soot mode, the particles will grow by coagulation (between the smaller particles) and condensational growth and are therefore not scavenged [207].

In Paper 2, the content of Zn, P and Ca in methanol and diesel did not exceed 2 ppm, while the sulfur content was 0.011 weight % for methanol, and 0.010 weight % for diesel. The effect of sulfur in the lubricity additive mixed with alcohols (Infineum R655) was negligible when compared with the sulfur content of engine lubricant.

It is therefore possible to rule out the possibility that the nanoparticles from alcohol combustion were primary (monomer) carbonaceous soot particles. The results in Figure 25 from the EDX analysis of a chosen single particle with a diameter of ~25 nm, which was similar to other observed nanoparticles with a diameter below 50

nm, showed peaks for Zn, Ca, S and P, previously found in lubrication oil. Additionally, oxygen, carbon, copper and silicon peaks were present in the particle analysis, but they presented artefacts from the TEM grid and the detector.
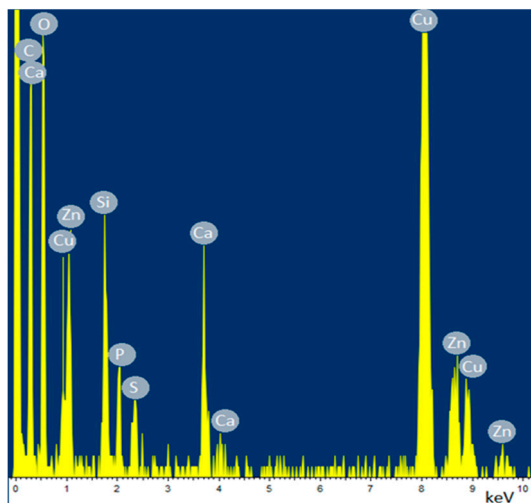
**Figure 25.** Results from the EDX analysis of a 25 nm nanoparticle from ethanol.

The results from the EDX analysis of diesel particles were similar to those from methanol and ethanol, also consisting of Zn, Ca, S and P. This was confirmed even in a later study on a different engine using fossil diesel fuel [148]. Large carbonaceous agglomerates, which were less abundant on the TEM grids collecting alcohol combustion particles, were more present with diesel. As mentioned in the previous section, a few large clusters of metallic nanoparticles consisting of the minerals from the lubrication oil, were only seen in the diesel sample.

The analysis of the particle phase organic aerosol in Paper 3, showed that there was a remarkable similarity between the mass spectral signatures of OA in PM from HVO and diesel fuels. The signature strongly resembled hydrocarbon-like organic aerosol mass spectra extracted from ambient datasets by e.g. traffic originated organic aerosol near roadside [208], probably due to a high abundance of lubrication oil dominating the mass spectra of the particles.

Despite strong similarities in the OA mass spectra between diesel and RME, there was a clear marker of tenfold intensity increase for RME exhaust at m/z 74 ($C_3H_6O_2^+$), possibly coming from the ester group in the FAME molecules. When quantifying the elemental composition (Figure 26), the difference between RME compared to diesel and HVO primary organic aerosol was reflected in a slightly higher O:C and a lower H:C ratio. The results were consistent with fuel contributions for the RME case, as the fatty acid methyl esters in RME have mass oxygen content of ~10.6%, compared to 0.2% in fossil diesel and no oxygen in HVO.

Oxygenated RME and non-aromatic HVO behaved somewhat differently in OA source appointment. Fresh OA from HVO was very similar to that of fossil diesel, but its SOA (aged OA) had higher O:C value and lower H:C value.

Finally, the DOC had a clear effect on chemical composition of OA in both fresh and aged exhaust from HVO combustion, see Figure 26. The DOC increased the average carbon oxidation state, by increasing O:C (for fresh: from 0.06 to 0.1; for aged, unchanged at 0.38) and decreasing H:C (fresh: 1.84 to 1.74, aged 1.47 to 1.44).
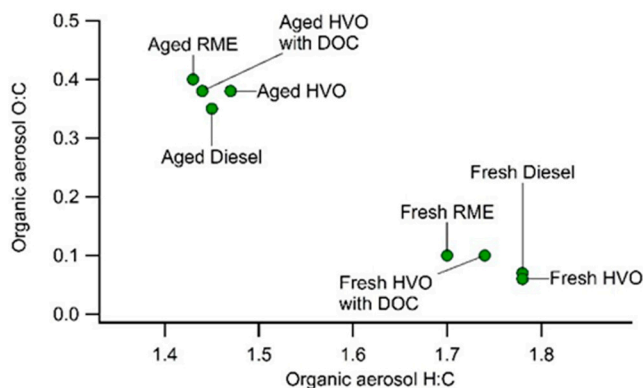
Figure 26. Overview of organic aerosol oxygen-to-carbon and hydrogen-to-carbon ratios for fresh and aged exhaust of diesel, RME and HVO.

Water uptake by an aerosol particle depends on the number of molecules and ions that it contributes to the aqueous phase. That is, it is favored by large size, low molar weight, high density, dissociation into ions and depends on the material being water-soluble. For these reasons the inorganic salts, as for example ammonium nitrate, show high hygroscopicity. For organic aerosol material, observations in [209] show an almost linear relation between the O:C ratio and the hygroscopicity [210]. The O:C ratio will therefore affect the water uptake in the atmosphere, which is central in predicting the direct climate effect of aerosols. Similarly, it also affects the ability of particles to act as cloud condensation nuclei (indirect aerosol effect on climate) [211]. This means that OA from RME emissions, with the highest O:C values of both OA and SOA among the fuels tested in Paper 3, had tendency to absorb slightly more moisture form the atmosphere and behave differently than fossil diesel exhaust OA and SOA. In the atmosphere, the organic aerosol emitted from combustion of the different fuels will be mixed with a pre-existing aerosol and be subject to condensation of vapors which are in many cases water soluble. It is thus not straightforward to tell if the emissions will increase the number of CCN by increasing the particle number or if the effect is the opposite due to the total aerosol material being distributed over a higher number of particles that could be too small to act as cloud condensation nuclei at the actual meteorological conditions.

6 Conclusion

6.1 Summary and conclusions

In order to contribute to defossilization of the transportation sector, a comprehensive literature study was done and experiments were performed on a single-cylinder heavy-duty engine. The effect of replacing fossil diesel fuel with renewable diesel-like and alcohol fuels on the engine performance and the pollutant emissions was investigated.

The main result of the research presented in this PhD thesis is that the organic fractions of the primary organic aerosol from HVO, RME and diesel combustion have engine lubrication oil signatures, whereas a clear fuel contribution to the organic mass spectra appears only in the emissions from RME combustion. Furthermore, nanoparticles in the exhaust from the combustion of light alcohols as well as diesel are also shown to originate from the constituents of the lubrication oil. Finally, diesel soot contains fly ashes which are products of combustion of the lubrication oil. This gives a strong indication of the influence of lubrication oil on the emissions.

RME reduces soot levels by a factor of two for low EGR levels, and by three to four for high EGR levels, when compared to fossil diesel. This opens a possibility to apply higher levels of EGR and stay in the region of low NOx, CO and THC emissions, while producing less soot than with diesel or B20. At all comparable EGR levels in the range from 0 to ~60%, RME has the lowest total particle number emissions, followed by B20 and diesel.

According to different studies [20][148][200], the relative impact of burned and unburned lubricating oil on the exhaust composition depends strongly on engine load and speed conditions. The results presented in this thesis show that emission factors of HC (gas phase) and OA (PM fraction of organics) are around three times lower for RME compared to diesel. In addition, the nucleation mode mass is shown in [49] to be lower for RME than diesel and HVO. Furthermore, fly ashes thought to originate from the burned engine lubrication oil droplets present in diesel emissions are not found in RME PM. This opens a new question on the oil slip or the oil layer on the cylinder liner being differently affected depending on the fuel, and in particular behaving differently for RME compared to fossil diesel. The reasons behind this are yet to be studied.

Simulated atmospheric aging of emissions strongly increases the organic aerosol for HVO and diesel, but the formation of secondary aerosol is considerably lower for RME. Primary organic emissions are strongly reduced in both the gas phase as THC, and in the particle phase measured as OA, after passing through a diesel oxidation catalyst. The DOC is also effective in reducing SOA formation upon atmospheric aging.

It is also demonstrated, by studying the influence of parameters controlling the E85 combustion processes on engine performance and emissions, that it may be possible to use commercially available alcohol-based E85 fuel in legacy engines with some modifications.

These results can be further developed as suggested in the next section.

6.2 Outlook

There is always a possibility for improvements to the experimental setup and methodology. Furthermore, there are numerous ideas about what can be studied in future to develop the aforementioned contributions into products or to expand the knowledge and use it for improving existing technology.

The experiments on which this PhD thesis was based were conducted on a one-cylinder engine. The results should be scalable to a multi-cylinder HD DICI engine. The findings are representing fundamental knowledge about the exhaust composition. They are, however, obtained at low and mid-to-low load engine operation and further experiments are needed to gain a broader knowledge about the trends over the full load range.

It would be particularly interesting to conduct a more detailed and fundamental study of the effect that fuel properties of RME have on in-cylinder processes and consequently on the organic fraction of PM, since it would provide valuable knowledge for understanding the contribution of lubrication oil to the emissions.

A practical improvement for the experimental setup when measuring unburned fuel in emissions from alcohol fuels would be to use a Fourier-transform infrared spectroscopy (FTIR) analyzer instead of a flame ionization detector (FID) which underestimates the emitted levels significantly in some cases. An FTIR can provide accurate measurements with alcohol fuels [212]. Even though these techniques are expensive and are less accessible compared to FID analyzers, the Engine Lab at Lund University will soon have them available for use.

It cannot be emphasized too strongly how important it is to utilize the available renewable fuels in the existing diesel engines in original configuration (with the necessary modifications) and bring them to the transportation market. This will lead

to considerable GHG emission savings in the short to medium term, while the long-term solutions are developed, and for the applications and areas where green electrification or other zero tailpipe emission options may not be technically feasible at scale. The earlier the savings can be made, the greater the overall savings that can be achieved to offset climate change. Decarbonization today dramatically reduces future challenges [213].

Acknowledgements

References

[1] The Editors of Encyclopaedia Britannica, "transportation," *Encyclopedia Britannica*. 2019. Accessed: Oct. 18, 2022. [Online]. Available: https://www.britannica.com/technology/transportation-technology

[2] UN General Assembly, *Transforming our world : the 2030 Agenda for Sustainable Development*. 2015. Accessed: Oct. 18, 2022. [Online]. Available: https://www.refworld.org/docid/57b6e3e44.html

[3] United Nations Sustainable Development Goals, "Communications materials." https://www.un.org/sustainabledevelopment/news/communications-material/ (accessed Nov. 27, 2022).

[4] P. Forster *et al.*, *Changes in Atmospheric Constituents and in Radiative Forcing Chapter 2*. United Kingdom: Cambridge University Press, 2007. [Online]. Available: http://inis.iaea.org/search/search.aspx?orig_q=RN:39002468

[5] S. Szopa *et al.*, "Short-Lived Climate Forcers. In Climate Change 2021: The Physical Science Basis. Contribution of Working Group I to the Sixth Assessment Report of the Intergovernmental Panel on Climate Change," 2021. doi: 10.1017/9781009157896.008.

[6] O. Wallach, "Race to Net Zero: Carbon Neutral Goals by Country," *Visual Capitalist*, 2022, Accessed: Oct. 18, 2022. [Online]. Available: https://www.visualcapitalist.com/sp/race-to-net-zero-carbon-neutral-goals-by-country/

[7] H. Ritchie, M. Roser, and P. Rosado, "CO_2 and Greenhouse Gas Emissions," *Our World in Data*, 2020, Accessed: Oct. 18, 2022. [Online]. Available: https://ourworldindata.org/emissions-by-sector

[8] H. Ritchie, "Cars, planes, trains: where do CO_2 emissions from transport come from?," *Our World in Data*, 2020, Accessed: Oct. 18, 2022. [Online]. Available: https://ourworldindata.org/co2-emissions-from-transport

[9] V. Smil, *Prime Movers of Globalization: The History and Impact of Diesel Engines and Gas Turbines*, Illustrated edition. The MIT Press, 2013.

[10] T. Wisell, M.-O. Larsson, C. Hult, and C. Fredricsson, "Korttidsprognoser för den svenska fordonsflottan – metoder och antaganden," 2019. Accessed: Oct. 19, 2022. [Online]. Available: https://www.ivl.se/download/18.694ca0617a1de98f473747/1628416911455/FULLTEXT01.pdf

[11] L. Thörn, "Vägfordonsflottans utveckling till år 2030," 2020. Accessed: Oct. 19, 2022. [Online]. Available: https://www.trafa.se/globalassets/pm/2020/pm-2020_7-vagfordonflottans-utveckling-till-ar-2030.pdf

[12] K. Senecal and F. Leach, *Racing Toward Zero: The Untold Story of Driving Green*. SAE International, 2021.

[13] H. Stripple, "Life Cycle Assessment of Road: A Pilot Study for Inventory Analysis," 2001. Accessed: Nov. 29, 2022. [Online]. Available: https://www.ivl.se/download/18.694ca0617a1de98f473458/1628416184474/FULLTEXT01.pdf

[14] A. A. Butt, S. Toller, and B. Birgisson, "Life cycle assessment for the green procurement of roads: a way forward," *J Clean Prod*, vol. 90, pp. 163–170, 2015, doi: 10.1016/j.jclepro.2014.11.068.

[15] Amnesty International, "'This Is What We Die For': Human Rights Abuses in the Democratic Republic of the Congo Power the Global Trade in Cobalt," 2016. Accessed: Oct. 25, 2022. [Online]. Available: https://www.amnesty.org/en/wp-content/uploads/2021/05/AFR6231832016ENGLISH.pdf

[16] M. Lightfoot, "Three steps to clean up electric vehicle supply chains," *World Economic Forum*, 2019. Accessed: Oct. 25, 2022. [Online]. Available: https://www.weforum.org/agenda/2019/09/clean-vehicles-have-a-dirty-secret-and-it-s-time-we-took-action/

[17] M. Alaküla and F. J. Márquez-Fernández, "Conductive electric road systems (ERs) in Sweden—An overview of development and testing activities," in *JSAE Annual Congress (Spring)*, 2019, pp. 1–8.

[18] F. J. Márquez-Fernández, J. Bischoff, G. Domingues-Olavarría, and M. Alaküla, "Assessment of Future EV Charging Infrastructure Scenarios for Long-Distance Transport in Sweden," *IEEE Trans Transp Electrification*, vol. 8, no. 1, pp. 615–626, 2022, doi: 10.1109/TTE.2021.3065144.

[19] R. Rezaei, C. Hayduk, A. Fandakov, M. Rieß, M. Sens, and T. O. Delebinski, "Numerical and Experimental Investigations of Hydrogen Combustion for Heavy-Duty Applications," *SAE Tech Pap*, 2021. doi: 10.4271/2021-01-0522.

[20] P. Tornehed and U. Olofsson, "Towards a Model for Engine Oil Hydrocarbon Particulate Matter," *SAE Int J Fuels Lubr*, vol. 3, no. 2, pp. 543–558, 2010, doi: 10.4271/2010-01-2098.

[21] S. Verhelst and T. Wallner, "Hydrogen-fueled internal combustion engines," *Prog Energy Combust Sci*, vol. 35, no. 6. pp. 490–527, 2009. doi: 10.1016/j.pecs.2009.08.001.

[22] C. Bekdemir, E. Doosje, and X. Seykens, "H_2-ICE Technology Options of the Present and the Near Future," *SAE Tech Pap*, 2022. doi: 10.4271/2022-01-0472.

[23] S. Verhelst, J. W. G. Turner, L. Sileghem, and J. Vancoillie, "Methanol as a fuel for internal combustion engines," *Prog Energy Combust Sci*, vol. 70, pp. 43–88, 2019, doi: 10.1016/j.pecs.2018.10.001.

[24] H. A. Alalwan, A. H. Alminshid, and H. A. S. Aljaafari, "Promising evolution of biofuel generations. Subject review," *Renew Energy Focus*, vol. 28, pp. 127–139, 2019, doi: 10.1016/j.ref.2018.12.006.

[25] A. Muscat, E. M. de Olde, I. J. M. de Boer, and R. Ripoll-Bosch, "The battle for biomass: A systematic review of food-feed-fuel competition," *Glob Food Sec*, vol. 25, p. 100330, 2020, doi: 10.1016/j.gfs.2019.100330.

[26] R. M. Handler *et al.*, "Evaluation of environmental impacts from microalgae cultivation in open-air raceway ponds: Analysis of the prior literature and investigation of wide variance in predicted impacts," *Algal Res*, vol. 1, no. 1, pp. 83–92, 2012, doi: 10.1016/j.algal.2012.02.003.

[27] R. A. Lee and J.-M. Lavoie, "From first- to third-generation biofuels: Challenges of producing a commodity from a biomass of increasing complexity," *Animal Frontiers*, vol. 3, no. 2, pp. 6–11, 2013, doi: 10.2527/af.2013-0010.

[28] L. J. France, P. P. Edwards, V. L. Kuznetsov, and H. Almegren, "Chapter 10 – The Indirect and Direct Conversion of CO_2 into Higher Carbon Fuels," in *Carbon Dioxide Utilisation*, P. Styring, E. A. Quadrelli, and K. Armstrong, Eds. Amsterdam: Elsevier, 2015, pp. 161–182. doi: 10.1016/B978-0-444-62746-9.00010-4.

[29] Z. Liu, K. Wang, Y. Chen, T. Tan, and J. Nielsen, "Third-generation biorefineries as the means to produce fuels and chemicals from CO_2," *Nat Catal*, vol. 3, no. 3, pp. 274–288, 2020, doi: 10.1038/s41929-019-0421-5.

[30] J. Lü, C. Sheahan, and P. Fu, "Metabolic engineering of algae for fourth generation biofuels production," *Energy Environ Sci*, vol. 4, no. 7, pp. 2451–2466, 2011, doi: 10.1039/C0EE00593B.

[31] V. S. Sikarwar, M. Zhao, P. S. Fennell, N. Shah, and E. J. Anthony, "Progress in biofuel production from gasification," *Prog Energy Combust Sci*, vol. 61, pp. 189–248, 2017, doi: 10.1016/j.pecs.2017.04.001.

[32] V. B. Malmborg *et al.*, "Evolution of In-Cylinder Diesel Engine Soot and Emission Characteristics Investigated with Online Aerosol Mass Spectrometry," *Environ Sci Technol*, vol. 51, no. 3, pp. 1876–1885, 2017, doi: 10.1021/acs.est.6b03391.

[33] Stockholms stad, "Diesel," 2022. https://hallbart.stockholm/lar-dig-mer/drivmedel-klimat/diesel/ (accessed Nov. 28, 2022).

[34] M. Lapuerta, O. Armas, and J. Rodríguez-Fernández, "Effect of biodiesel fuels on diesel engine emissions," *Prog Energy Combust Sci*, vol. 34, no. 2, pp. 198–223, 2008, doi: 10.1016/j.pecs.2007.07.001.

[35] J. Sun, J. A. Caton, and T. J. Jacobs, "Oxides of nitrogen emissions from biodiesel-fuelled diesel engines," *Prog Energy Combust Sci*, vol. 36, no. 6, pp. 677–695, 2010. doi: 10.1016/j.pecs.2010.02.004.

[36] G. Karavalakis, K. C. Johnson, M. Hajbabaei, and T. D. Durbin, "Application of low-level biodiesel blends on heavy-duty (diesel) engines: Feedstock implications on NOx and particulate emissions," *Fuel*, vol. 181, pp. 259–268, 2016, doi: 10.1016/j.fuel.2016.05.001.

[37] D. Kim, S. Kim, S. Oh, and S.-Y. No, "Engine performance and emission characteristics of hydrotreated vegetable oil in light duty diesel engines," *Fuel*, vol. 125, pp. 36–43, 2014, doi: 10.1016/j.fuel.2014.01.089.

[38] H. Aatola, M. Larmi, T. Sarjovaara, and S. Mikkonen, "Hydrotreated Vegetable Oil (HVO) as a Renewable Diesel Fuel: Trade-off between NOx, Particulate Emission, and Fuel Consumption of a Heavy Duty Engine," *SAE Int J Engines*, vol. 1, no. 1, pp. 1251–1262, 2009, doi: 10.4271/2008-01-2500.

[39] M. Kuronen, S. Mikkonen, P. Aakko, and T. Murtonen, "Hydrotreated Vegetable Oil as Fuel for Heavy Duty Diesel Engines," *SAE Tech Pap*, 2007. doi: 10.4271/2007-01-4031.

[40] Neste Corporation, "Neste renewable diesel handbook," 2020. Accessed: Nov. 03, 2022. [Online]. Available: https://www.neste.com/sites/default/files/attachments/neste_renewable_diesel_handbook.pdf

[41] G. Knothe, "Biodiesel and renewable diesel: A comparison," *Prog Energy Combust Sci*, vol. 36, no. 3, pp. 364–373, 2010, doi: 10.1016/j.pecs.2009.11.004.

[42] M. Lapuerta, M. Villajos, J. R. Agudelo, and A. L. Boehman, "Key properties and blending strategies of hydrotreated vegetable oil as biofuel for diesel engines," *Fuel Process Technol*, vol. 92, no. 12, pp. 2406–2411, 2011, doi: 10.1016/j.fuproc.2011.09.003.

[43] P. Šimáček, D. Kubička, I. Kubičková, F. Homola, M. Pospíšil, and J. Chudoba, "Premium quality renewable diesel fuel by hydroprocessing of sunflower oil," *Fuel*, vol. 90, no. 7, pp. 2473–2479, 2011, doi: 10.1016/j.fuel.2011.03.013.

[44] P. Šimáček, D. Kubička, G. Šebor, and M. Pospíšil, "Fuel properties of hydroprocessed rapeseed oil," *Fuel*, vol. 89, no. 3, pp. 611–615, 2010, doi: 10.1016/j.fuel.2009.09.017.

[45] E. G. Giakoumis, C. D. Rakopoulos, A. M. Dimaratos, and D. C. Rakopoulos, "Exhaust emissions of diesel engines operating under transient conditions with biodiesel fuel blends," *Prog Energy Combust Sci*, vol. 38, no. 5, pp. 691–715, 2012, doi: 10.1016/j.pecs.2012.05.002.

[46] C. McCaffery, G. Karavalakis, T. Durbin, H. Jung, and K. Johnson, "Engine-Out Emissions Characteristics of a Light Duty Vehicle Operating on a Hydrogenated Vegetable Oil Renewable Diesel," *SAE Tech Pap*, 2020. doi: 10.4271/2020-01-0337.

[47] N. Savic *et al.*, "Influence of biodiesel fuel composition on the morphology and microstructure of particles emitted from diesel engines," *Carbon*, vol. 104, pp. 179–189, 2016, doi: 10.1016/j.carbon.2016.03.061.

[48] H. Xu, L. Ou, Y. Li, T. R. Hawkins, and M. Wang, "Life Cycle Greenhouse Gas Emissions of Biodiesel and Renewable Diesel Production in the United States," *Environ Sci Technol*, vol. 56, no. 12, pp. 7512–7521, 2022, doi: 10.1021/acs.est.2c00289.

[49] L. Gren *et al.*, "Effects of renewable fuel and exhaust aftertreatment on primary and secondary emissions from a modern heavy-duty diesel engine," *J Aerosol Sci*, vol. 156, 2021, doi: 10.1016/j.jaerosci.2021.105781.

[50] McKinsey & Company, "McKinsey Energy Insights Executive Summary: Global Energy Perspective 2022," 2022, Accessed: Oct. 7, 2022. [Online]. Available: https://www.mckinsey.com/industries/oil-and-gas/our-insights/global-energy-perspective-2022

[51] M. Tuner, "Review and Benchmarking of Alternative Fuels in Conventional and Advanced Engine Concepts with Emphasis on Efficiency, CO₂ , and Regulated Emissions," *SAE Tech Pap*, 2016. doi: 10.4271/2016-01-0882.

[52] C. Esarte, M. Abián, Á. Millera, R. Bilbao, and M. U. Alzueta, "Gas and soot products formed in the pyrolysis of acetylene mixed with methanol, ethanol, isopropanol or n-butanol," *Energy*, vol. 43, no. 1, pp. 37–46, 2012, doi: 10.1016/j.energy.2011.11.027.

[53] H. O. Hardenberg and A. J. Schaefer, "The Use of Ethanol as a Fuel for Compression Ignition Engines," *SAE Tech Pap*, 1981. doi: 10.4271/811211.

[54] B. Gainey, Z. Yan, J. Gandolfo, and B. Lawler, "Methanol and wet ethanol as interchangeable fuels for internal combustion engines: LCA, TEA, and experimental comparison," *Fuel*, vol. 333, p. 126257, 2023, doi: 10.1016/j.fuel.2022.126257.

[55] Energimyndigheten, "Drivmedel 2020: Redovisning av rapporterade uppgifter enligt drivmedelslagen, hållbarhetslagen och reduktionsplikten," 2021, Accessed: Oct. 11, 2022. [Online]. Available: https://energimyndigheten.a-w2m.se/FolderContents.mvc/Download?ResourceId=203063

[56] P. Aakko-Saksa, L. Rantanen-Kolehmainen, P. Koponen, A. Engman, and J. Kihlman, "Biogasoline Options - Possibilities for Achieving High Bio-share and Compatibility with Conventional Cars," *SAE Int J Fuels Lubr*, vol. 4, no. 2, 2011, doi: 10.4271/2011-24-0111.

[57] M. Kaiadi, B. Johansson, M. Lundgren, and J. A. Gaynor, "Sensitivity Analysis Study on Ethanol Partially Premixed Combustion," *SAE Int J Engines*, vol. 6, no. 1, 2013, doi: 10.4271/2013-01-0269.

[58] G. T. Kalghatgi, P. Risberg, and H.-E. Angstrom, "Partially Pre-Mixed Auto-Ignition of Gasoline to Attain Low Smoke and Low NOx at High Load in a Compression Ignition Engine and Comparison with a Diesel Fuel," *SAE Tech Pap*, 2007. doi: 10.4271/2007-01-0006.

[59] V. Manente, B. Johansson, and P. Tunestal, "Characterization of Partially Premixed Combustion With Ethanol: EGR Sweeps, Low and Maximum Loads," in *ASME 2009 Internal Combustion Engine Division Spring Technical Conference*, 2009, pp. 175–190. doi: 10.1115/ICES2009-76165.

[60] V. Manente, B. Johansson, and P. Tunestal, "Partially Premixed Combustion at High Load using Gasoline and Ethanol, a Comparison with Diesel," *SAE Tech Pap*, 2009. doi: 10.4271/2009-01-0944.

[61] M. H. L. Silveira, B. A. Vanelli, and A. K. Chandel, "Chapter 6 - Second Generation Ethanol Production: Potential Biomass Feedstock, Biomass Deconstruction, and Chemical Platforms for Process Valorization," in *Advances in Sugarcane Biorefinery*, A. K. Chandel and M. H. Luciano Silveira, Eds. Elsevier, 2018, pp. 135–152. doi: 10.1016/B978-0-12-804534-3.00006-9.

[62] A. Goeppert, M. Czaun, J.-P. Jones, G. K. Surya Prakash, and G. A. Olah, "Recycling of carbon dioxide to methanol and derived products – closing the loop," *Chem Soc Rev*, vol. 43, no. 23, pp. 7995–8048, 2014, doi: 10.1039/C4CS00122B.

[63] J. A. Martens *et al.*, "The Chemical Route to a Carbon Dioxide Neutral World," *ChemSusChem*, vol. 10, no. 6, pp. 1039–1055, 2017, doi: 10.1002/cssc.201601051.

[64] C. Schweitzer, "Synthesizing strengths of 1st and 3rd generation biorefineries. Biomethanol as a biorefinery product," *Int Sugar J*, vol. 116, no. 1390, pp. 766–772, 2014.

[65] M. Svensson, M. Tuner, and S. Verhelst, "Low Load Ignitability of Methanol in a Heavy-Duty Compression Ignition Engine," *SAE Tech Pap*, 2022, doi: 10.4271/2022-01-1093.

[66] The European Commission, *Renewable Energy Directive (REDII)*. 2018.

[67] C. Malins, "Beyond biomass? Alternative fuels from renewable electricity and carbon recycling," 2020. Accessed: Oct. 22, 2022. [Online]. Available: https://theicct.org/wp-content/uploads/2021/06/Cerulogy_Beyond-Biomass_May2020_0.pdf

[68] The European Biodiesel Board, "Parliament vote confirms critical role of sustainable biodiesel for the EU Climate Objectives," 2022. https://ebb-eu.org/news/parliament-vote-confirms-critical-role-of-sustainable-biodiesel-for-the-eu-climate-objectives/ (accessed Oct. 24, 2022)

[69] The European Commission, "Renewable energy directive," 2022. https://energy.ec.europa.eu/topics/renewable-energy/renewable-energy-directive-targets-and-rules/renewable-energy-directive_en (accessed Oct. 24, 2022).

[70] B. Giechaskiel, A. Melas, G. Martini, P. Dilara, and L. Ntziachristos, "Revisiting Total Particle Number Measurements for Vehicle Exhaust Regulations," *Atmosphere*, vol. 13, no. 2, 2022, doi: 10.3390/atmos13020155.

[71] B. Giechaskiel, "Solid Particle Number Emission Factors of Euro VI Heavy-Duty Vehicles on the Road and in the Laboratory," *Int J Environ Res Public Health*, vol. 15, no. 2, 2018, doi: 10.3390/ijerph15020304.

[72] UNECE, *Global technical regulation (GTR) No. 4 - Test Procedure for Compression-Ignition (C.I.) Engines and Positive-Ignition (P.I.) Engines Fuelled with Natural Gas (NG) or Liquefied Petroleum Gas (LPG) with Regard to the Emission of Pollutants*. Switzerland, 2007.

[73] UNECE, *ANNEXES to the Proposal for a Regulation of the European Parliament and the Council on type-approval of motor vehicles and engines and of systems, components and separate technical units intended for such vehicles, with respect to their emissions and battery durability (Euro 7)*. 2022.

[74] UNECE, *Proposal for the REGULATION OF THE EUROPEAN PARLIAMENT AND OF THE COUNCIL on type-approval of motor vehicles and engines and of systems, components and separate technical units intended for such vehicles, with respect to their emissions and battery durability (Euro 7)*. 2022.

[75] H. Timonen *et al.*, "Influence of fuel ethanol content on primary emissions and secondary aerosol formation potential for a modern flex-fuel gasoline vehicle," *Atmos Chem Phys*, vol. 17, no. 8, pp. 5311–5329, 2017, doi: 10.5194/acp-17-5311-2017.

[76] L. Gren *et al.*, "Effect of Renewable Fuels and Intake O_2 Concentration on Diesel Engine Emission Characteristics and Reactive Oxygen Species (ROS) Formation," *Atmosphere*, vol. 11, no. 6, 2020, doi: 10.3390/atmos11060641.

[77] M. Gustafsson, J. Lindén, B. Forsberg, S. Åström, and E. Johansson, "Quantification of population exposure to NO₂, PM2.5 and PM10 and estimated health impacts 2019," 2022. Accessed: Dec. 03, 2022. [Online]. Available: https://www.ivl.se/download/18.77932582182575f4af3ff14/1667990828671/2446.pdf

[78] European Environment Agency (EEA), "Air quality in Europe 2022," 2022, Accessed: Dec. 03, 2022. [Online]. Available: https://www.eea.europa.eu/publications/air-quality-in-europe-2022

[79] World Health Organization, *WHO global air quality guidelines: particulate matter (PM2.5 and PM10), ozone, nitrogen dioxide, sulfur dioxide and carbon monoxide*. Geneva: World Health Organization, 2021. [Online]. Available: https://apps.who.int/iris/handle/10665/345329

[80] J. E. Dec, "Advanced compression-ignition engines—understanding the in-cylinder processes," *Proc Combus Inst*, vol. 32, no. 2, pp. 2727–2742, 2009, doi: 10.1016/j.proci.2008.08.008.

[81] S. L. Winkler, J. E. Anderson, L. Garza, W. C. Ruona, R. Vogt, and T. J. Wallington, "Vehicle criteria pollutant (PM, NOx, CO, HCs) emissions: how low should we go?," *NPJ Clim Atmos Sci*, vol. 1, no. 1, p. 26, 2018, doi: 10.1038/s41612-018-0037-5.

[82] D. Saadi, E. Tirosh, and I. Schnell, "The Relationship between City Size and Carbon Monoxide (CO) Concentration and Their Effect on Heart Rate Variability (HRV).," *Int J Environ Res Public Health*, vol. 18, no. 2, 2021, doi: 10.3390/ijerph18020788.

[83] Texas Commission on Environmental Quality, "Air Pollution from Carbon Monoxide," 2022. https://www.tceq.texas.gov/airquality/sip/criteria-pollutants/sip-co (accessed Nov. 27, 2022).

[84] First Alert, "What levels of carbon monoxide (CO) will cause an alarm?" https://support.firstalert.com/s/article/What-levels-of-carbon-monoxide-CO-will-cause-an-alarm (accessed Dec. 02, 2022).

[85] X. Han and L. P. Naeher, "A review of traffic-related air pollution exposure assessment studies in the developing world," *Environ Int*, vol. 32, no. 1, pp. 106–120, 2006, doi: 10.1016/j.envint.2005.05.020.

[86] J. de Gouw and J. L. Jimenez, "Organic aerosols in the earth's atmosphere," *Environ Sci Technol*, vol. 43, no. 20. pp. 7614–7618, 2009. doi: 10.1021/es9006004.

[87] J. Sun and P. A. Ariya, "Atmospheric organic and bio-aerosols as cloud condensation nuclei (CCN): A review," *Atmos Environ*, vol. 40, no. 5. pp. 795–820, 2006. doi: 10.1016/j.atmosenv.2005.05.052.

[88] T. Rönkkö and H. Timonen, "Overview of Sources and Characteristics of Nanoparticles in Urban Traffic-Influenced Areas," *J Alzheimer's Dis*, vol. 72, pp. 15–28, 2019, doi: 10.3233/JAD-190170.

[89] P. J. Adams and J. H. Seinfeld, "Predicting global aerosol size distributions in general circulation models," *J Geophys Res Atmos*, vol. 107, no. D19, p. AAC 4-1-AAC 4-23, 2002, doi: 10.1029/2001JD001010.

[90] G. Oberdörster, E. Oberdörster, and J. Oberdörster, "Nanotoxicology: an emerging discipline evolving from studies of ultrafine particles.," *Environ Health Perspect*, vol. 113, no. 7, pp. 823–39, 2005, doi: 10.1289/ehp.7339.

[91] J. Heyder, J. Gebhart, G. Rudolf, C. F. Schiller, and W. Stahlhofen, "Deposition of particles in the human respiratory tract in the size range 0.005–15 µm," *J Aerosol Sci*, vol. 17, no. 5, pp. 811–825, 1986, doi: 10.1016/0021-8502(86)90035-2.

[92] Y.-F. Xing, Y.-H. Xu, M.-H. Shi, and Y.-X. Lian, "The impact of PM2.5 on the human respiratory system.," *J Thorac Dis*, vol. 8, no. 1, pp. E69-74, 2016, doi: 10.3978/j.issn.2072-1439.2016.01.19.

[93] T. Lepistö, H. Kuuluvainen, P. Juuti, A. Järvinen, A. Arffman, and T. Rönkkö, "Measurement of the human respiratory tract deposited surface area of particles with an electrical low pressure impactor," *Aerosol Sci Technol*, vol. 54, no. 8, pp. 958–971, 2020, doi: 10.1080/02786826.2020.1745141.

[94] P. J. A. Borm, R. P. F. Schins, and C. Albrecht, "Inhaled particles and lung cancer, part B: Paradigms and risk assessment," *Int J Cancer*, vol. 110, no. 1, pp. 3–14, 2004, doi: 10.1002/ijc.20064.

[95] C. Ostiguy, B. Soucy, G. Lapointe, C. Woods, L. Ménard, and M. Trottier, "Health Effects of Nanoparticles, Second Edition." 2006.

[96] D. Kittelson, I. Khalek, J. McDonald, J. Stevens, and R. Giannelli, "Particle emissions from mobile sources: Discussion of ultrafine particle emissions and definition," *J Aerosol Sci*, vol. 159, p. 105881, 2022, doi: 10.1016/j.jaerosci.2021.105881.

[97] L. Morawska, Z. Ristovski, E. R. Jayaratne, D. U. Keogh, and X. Ling, "Ambient nano and ultrafine particles from motor vehicle emissions: Characteristics, ambient processing and implications on human exposure," *Atmos Environ*, vol. 42, no. 35, pp. 8113–8138, 2008, doi: 10.1016/j.atmosenv.2008.07.050.

[98] J.-H. Tsai, S.-Y. Chang, and H.-L. Chiang, "Volatile organic compounds from the exhaust of light-duty diesel vehicles," *Atmos Environ*, vol. 61, pp. 499–506, 2012, doi: 10.1016/j.atmosenv.2012.07.078.

[99] T. Rönkkö *et al.*, "Effects of gaseous sulphuric acid on diesel exhaust nanoparticle formation and characteristics," *Environmental science & technology*, vol. 47, no. 20, p. 11882—11889, doi: 10.1021/es402354y.

[100] T. C. Pederson and J.-S. Siak, "The role of nitroaromatic compounds in the direct-acting mutagenicity of diesel particle extracts," *J Appl Toxicol*, vol. 1, no. 2, pp. 54–60, 1981, doi: 10.1002/jat.2550010203.

[101] A. H. Miguel, T. W. Kirchstetter, R. A. Harley, and S. v Hering, "On-Road Emissions of Particulate Polycyclic Aromatic Hydrocarbons and Black Carbon from Gasoline and Diesel Vehicles," *Environ Sci Technol*, vol. 32, no. 4, pp. 450–455, 1998, doi: 10.1021/es970566w.

[102] L. Kuusimäki, K. Peltonen, P. Mutanen, and K. Savela, "Analysis of Particle and Vapour Phase PAHs from the Personal Air Samples of Bus Garage Workers Exposed to Diesel Exhaust," *Ann Occup Hyg*, vol. 47, no. 5, pp. 389–398, 2003, doi: 10.1093/annhyg/meg037.

[103] B. A. A. L. van Setten, M. Makkee, and J. A. Moulijn, "Science and technology of catalytic diesel particulate filters," *Catal Rev Sci Eng*, vol. 43, no. 4, pp. 489–564, 2001, doi: 10.1081/CR-120001810.

[104] M. Matti Maricq, "Chemical characterization of particulate emissions from diesel engines: A review," *J Aerosol Sci*, vol. 38, no. 11, pp. 1079–1118, 2007, doi: 10.1016/j.jaerosci.2007.08.001.

[105] C. Ma *et al.*, "Transient Characterization of Automotive Exhaust Emission from Different Vehicle Types Based on On-Road Measurements," *Atmosphere*, vol. 11, no. 1, 2020, doi: 10.3390/atmos11010064.

[106] S. J. Harris and M. M. Maricq, "Signature size distributions for diesel and gasoline engine exhaust particulate matter," *J Aerosol Sci*, vol. 32, no. 6, pp. 749–764, 2001, doi: 10.1016/S0021-8502(00)00111-7.

[107] D. B. Kittelson, "Engines and nanoparticles: a review," *J Aerosol Sci*, vol. 29, no. 5, pp. 575–588, 1998, doi: 10.1016/S0021-8502(97)10037-4.

[108] M. M. Maricq, R. E. Chase, N. Xu, and P. M. Laing, "The Effects of the Catalytic Converter and Fuel Sulfur Level on Motor Vehicle Particulate Matter Emissions: Light Duty Diesel Vehicles," *Environ Sci Technol*, vol. 36, no. 2, pp. 283–289, 2002, doi: 10.1021/es010962l.

[109] B. Wang *et al.*, "Chemical and toxicological characterization of particulate emissions from diesel vehicles.," *J Hazard Mater*, vol. 405, p. 124613, 2021, doi: 10.1016/j.jhazmat.2020.124613.

[110] J. Xing *et al.*, "Morphology and composition of particles emitted from a port fuel injection gasoline vehicle under real-world driving test cycles," *J Environ Sci*, vol. 76, pp. 339–348, 2019, doi: 10.1016/j.jes.2018.05.026.

[111] A. Polidori, S. Hu, S. Biswas, R. J. Delfino, and C. Sioutas, "Real-time characterization of particle-bound polycyclic aromatic hydrocarbons in ambient aerosols and from motor-vehicle exhaust," *Atmos Chem Phys*, vol. 8, no. 5, pp. 1277–1291, 2008, doi: 10.5194/acp-8-1277-2008.

[112] D. D. Dutcher *et al.*, "Emissions from Ethanol-Gasoline Blends: A Single Particle Perspective," *Atmosphere*, vol. 2, no. 2, pp. 182–200, 2011, doi: 10.3390/atmos2020182.

[113] M. G. Perrone *et al.*, "Exhaust emissions of polycyclic aromatic hydrocarbons, n-alkanes and phenols from vehicles coming within different European classes," *Atmos Environ*, vol. 82, pp. 391–400, 2014, doi: 10.1016/j.atmosenv.2013.10.040.

[114] X. Cao, X. Hao, X. Shen, X. Jiang, B. Wu, and Z. Yao, "Emission characteristics of polycyclic aromatic hydrocarbons and nitro-polycyclic aromatic hydrocarbons from diesel trucks based on on-road measurements," *Atmos Environ*, vol. 148, pp. 190–196, 2017, doi: 10.1016/j.atmosenv.2016.10.040.

[115] T. Rönkkö *et al.*, "Traffic is a major source of atmospheric nanocluster aerosol," *Proceedings of the National Academy of Sciences*, vol. 114, no. 29, pp. 7549–7554, 2017, doi: 10.1073/pnas.1700830114.

[116] S.-B. Kwon, Ken. W. Lee, K. Saito, O. Shinozaki, and T. Seto, "Size-Dependent Volatility of Diesel Nanoparticles: Chassis Dynamometer Experiments," *Environ Sci Technol*, vol. 37, no. 9, pp. 1794–1802, 2003, doi: 10.1021/es025868z.

[117] T. Rönkkö, A. Virtanen, J. Kannosto, J. Keskinen, M. Lappi, and L. Pirjola, "Nucleation Mode Particles with a Nonvolatile Core in the Exhaust of a Heavy Duty Diesel Vehicle," *Environ Sci Technol*, vol. 41, no. 18, pp. 6384–6389, 2007, doi: 10.1021/es0705339.

[118] H. Kuuluvainen *et al.*, "Nonvolatile ultrafine particles observed to form trimodal size distributions in non-road diesel engine exhaust," *Aerosol Sci Technol*, vol. 54, no. 11, pp. 1345–1358, 2020, doi: 10.1080/02786826.2020.1783432.

[119] A. G. Sappok and V. W. Wong, "Detailed Chemical and Physical Characterization of Ash Species in Diesel Exhaust Entering Aftertreatment Systems," *SAE Tech Pap*, 2007. doi: 10.4271/2007-01-0318.

[120] A. Mayer, J. Czerwinski, M. Kasper, A. Ulrich, and J. J. Mooney, "Metal oxide particle emissions from diesel and petrol engines," *SAE Tech Pap*, 2012. doi: 10.4271/2012-01-0841.

[121] U. Kirchner, V. Scheer, R. Vogt, and R. Kägi, "TEM study on volatility and potential presence of solid cores in nucleation mode particles from diesel powered passenger cars," *J Aerosol Sci*, vol. 40, no. 1, pp. 55–64, 2009, doi: 10.1016/j.jaerosci.2008.08.002.

[122] A. de Filippo and M. M. Maricq, "Diesel Nucleation Mode Particles: Semivolatile or Solid?," *Environ Sci Technol*, vol. 42, no. 21, pp. 7957–7962, 2008, doi: 10.1021/es8010332.

[123] T. Rönkkö *et al.*, "Vehicle Engines Produce Exhaust Nanoparticles Even When Not Fueled," *Environ Sci Technol*, vol. 48, no. 3, pp. 2043–2050, 2014, doi: 10.1021/es405687m.

[124] M. Sirignano and A. D'Anna, "Filtration and coagulation efficiency of sub-10 nm combustion-generated particles," *Fuel*, vol. 221, pp. 298–302, 2018, doi: 10.1016/j.fuel.2018.02.107.

[125] A. Liati, A. Spiteri, P. Dimopoulos Eggenschwiler, and N. Vogel-Schäuble, "Microscopic investigation of soot and ash particulate matter derived from biofuel and diesel: implications for the reactivity of soot," *J Nanopart Res*, vol. 14, no. 11, p. 1224, 2012, doi: 10.1007/s11051-012-1224-7.

[126] D. Uy, J. Storey, C. S. Sluder, T. Barone, S. Lewis, and M. Jagner, "Effects of Oil Formulation, Oil Separator, and Engine Speed and Load on the Particle Size, Chemistry, and Morphology of Diesel Crankcase Aerosols," *SAE Int J Fuels Lubr*, vol. 9, no. 1, pp. 224–238, 2016, doi: 10.4271/2016-01-0897.

[127] U. Uhrner *et al.*, "Volatile Nanoparticle Formation and Growth within a Diluting Diesel Car Exhaust," *J Air Waste Manage Assoc*, vol. 61, no. 4, pp. 399–408, 2011, doi: 10.3155/1047-3289.61.4.399.

[128] A. Charron and R. M. Harrison, "Primary particle formation from vehicle emissions during exhaust dilution in the roadside atmosphere," *Atmos Environ*, vol. 37, no. 29, pp. 4109–4119, 2003, doi: 10.1016/S1352-2310(03)00510-7.

[129] R. Casati, V. Scheer, R. Vogt, and T. Benter, "Measurement of nucleation and soot mode particle emission from a diesel passenger car in real world and laboratory in situ dilution," *Atmos Environ*, vol. 41, no. 10, pp. 2125–2135, 2007, doi: 10.1016/j.atmosenv.2006.10.078.

[130] D. B. Kittelson *et al.*, "On-road evaluation of two Diesel exhaust aftertreatment devices," *J Aerosol Sci*, vol. 37, no. 9, pp. 1140–1151, 2006, doi: 10.1016/j.jaerosci.2005.11.003.

[131] L. Zhou *et al.*, "A transition of atmospheric emissions of particles and gases from on-road heavy-duty trucks," *Atmos Chem Phys*, vol. 20, no. 3, pp. 1701–1722, 2020, doi: 10.5194/acp-20-1701-2020.

[132] K. Vaaraslahti, A. Virtanen, J. Ristimäki, and J. Keskinen, "Nucleation Mode Formation in Heavy-Duty Diesel Exhaust with and without a Particulate Filter," *Environ Sci Technol*, vol. 38, no. 18, pp. 4884–4890, 2004, doi: 10.1021/es0353255.

[133] B. Giechaskiel, L. Ntziachristos, Z. Samaras, V. Scheer, R. Casati, and R. Vogt, "Formation potential of vehicle exhaust nucleation mode particles on-road and in the laboratory," *Atmos Environ*, vol. 39, no. 18, pp. 3191–3198, 2005, doi: 10.1016/j.atmosenv.2005.02.019.

[134] P. H. McMurry and S. K. Friedlander, "New particle formation in the presence of an aerosol," *Atmos Environ (1967)*, vol. 13, no. 12, pp. 1635–1651, 1979, doi: 10.1016/0004-6981(79)90322-6.

[135] D. M. Murphy *et al.*, "Single-particle mass spectrometry of tropospheric aerosol particles," *J Geophys Res Atmos*, vol. 111, no. D23, 2006, doi: 10.1029/2006JD007340.

[136] Q. Zhang *et al.*, "Ubiquity and dominance of oxygenated species in organic aerosols in anthropogenically-influenced Northern Hemisphere midlatitudes," *Geophys Res Lett*, vol. 34, no. 13, 2007, doi: 10.1029/2007GL029979.

[137] M. Hallquist *et al.*, "The formation, properties and impact of secondary organic aerosol: current and emerging issues," *Atmos Chem Phys*, vol. 9, no. 14, pp. 5155–5236, 2009, doi: 10.5194/acp-9-5155-2009.

[138] P. Roth *et al.*, "Intermediate and high ethanol blends reduce secondary organic aerosol formation from gasoline direct injection vehicles," *Atmos Environ*, vol. 220, p. 117064, 2020, doi: 10.1016/j.atmosenv.2019.117064.

[139] P. Karjalainen *et al.*, "Time-resolved characterization of primary particle emissions and secondary particle formation from a modern gasoline passenger car," *Atmos Chem Phys*, vol. 16, no. 13, pp. 8559–8570, 2016, doi: 10.5194/acp-16-8559-2016.

[140] W. Deng *et al.*, "Primary particulate emissions and secondary organic aerosol (SOA) formation from idling diesel vehicle exhaust in China.," *Sci Total Environ*, vol. 593–594, pp. 462–469, 2017, doi: 10.1016/j.scitotenv.2017.03.088.

[141] Q. Zhu *et al.*, "Improved source apportionment of organic aerosols in complex urban air pollution using the multilinear engine (ME-2)," *Atmos Meas Tech*, vol. 11, no. 2, pp. 1049–1060, 2018, doi: 10.5194/amt-11-1049-2018.

[142] P. Karjalainen *et al.*, "Strategies To Diminish the Emissions of Particles and Secondary Aerosol Formation from Diesel Engines," *Environ Sci Technol*, vol. 53, no. 17, pp. 10408–10416, 2019, doi: 10.1021/acs.est.9b04073.

[143] G. Karavalakis, T. D. Durbin, J. Yang, L. Ventura, and K. Xu, "Fuel Effects on PM Emissions from Different Vehicle/Engine Configurations: A Literature Review," *SAE Tech Pap*, 2018. doi: 10.4271/2018-01-0349.

[144] J. Yang, P. Roth, H. Zhu, T. D. Durbin, and G. Karavalakis, "Impacts of gasoline aromatic and ethanol levels on the emissions from GDI vehicles: Part 2. Influence on particulate matter, black carbon, and nanoparticle emissions," *Fuel*, vol. 252, pp. 812–820, 2019, doi: 10.1016/j.fuel.2019.04.144.

[145] M. Muñoz *et al.*, "Bioethanol Blending Reduces Nanoparticle, PAH, and Alkyl- and Nitro-PAH Emissions and the Genotoxic Potential of Exhaust from a Gasoline Direct Injection Flex-Fuel Vehicle," *Environ Sci Technol*, vol. 50, no. 21, pp. 11853–11861, 2016, doi: 10.1021/acs.est.6b02606.

[146] E. Distaso, R. Amirante, G. Calò, P. de Palma, and P. Tamburrano, "Evolution of Soot Particle Number, Mass and Size Distribution along the Exhaust Line of a Heavy-Duty Engine Fueled with Compressed Natural Gas," *Energies*, vol. 13, no. 15, 2020, doi: 10.3390/en13153993.

[147] M. R. Canagaratna *et al.*, "Chase Studies of Particulate Emissions from in-use New York City Vehicles," *Aeroso Sci Technol*, vol. 38, no. 6, pp. 555–573, 2004, doi: 10.1080/02786820490465504.

[148] S. Carbone *et al.*, "Distinguishing fuel and lubricating oil combustion products in diesel engine exhaust particles," *Aerosol Sci Technol*, vol. 53, no. 5, pp. 594–607, 2019, doi: 10.1080/02786826.2019.1584389.

[149] M. le Breton, M. Psichoudaki, M. Hallquist, Å. K. Watne, A. Lutz, and Å. M. Hallquist, "Application of a FIGAERO ToF CIMS for on-line characterization of real-world fresh and aged particle emissions from buses," *Aerosol Sci Technol* vol. 53, no. 3, pp. 244–259, 2019, doi: 10.1080/02786826.2019.1566592.

[150] C. Tomasi, S. Fuzzi, and A. Kokhanovsky, Eds., "Atmospheric Aerosols: Life Cycles and Effects on Air Quality and Climate," Berlin: Wiley-VCH, 2017.

[151] K. Gorkowski, N. M. Donahue, and R. C. Sullivan, "Aerosol Optical Tweezers Constrain the Morphology Evolution of Liquid-Liquid Phase-Separated Atmospheric Particles," *Chem*, vol. 6, no. 1, pp. 204–220, 2020, doi: 10.1016/j.chempr.2019.10.018.

[152] R. Volkamer *et al.*, "Secondary organic aerosol formation from anthropogenic air pollution: Rapid and higher than expected," *Geophys Res Lett*, vol. 33, no. 17, 2006, doi: 10.1029/2006GL026899.

[153] V. A. Lanz, M. R. Alfarra, U. Baltensperger, B. Buchmann, C. Hueglin, and A. S. H. Prévôt, "Source apportionment of submicron organic aerosols at an urban site by factor analytical modelling of aerosol mass spectra," *Atmos Chem Phys*, vol. 7, no. 6, pp. 1503–1522, 2007, doi: 10.5194/acp-7-1503-2007.

[154] E. Z. Nordin *et al.*, "Secondary organic aerosol formation from idling gasoline passenger vehicle emissions investigated in a smog chamber," *Atmos Chem Phys*, vol. 13, no. 12, pp. 6101–6116, 2013, doi: 10.5194/acp-13-6101-2013.

[155] J. Ye *et al.*, "Predicting Secondary Organic Aerosol Enhancement in the Presence of Atmospherically Relevant Organic Particles," *ACS Earth Space Chem*, vol. 2, no. 10, pp. 1035–1046, 2018, doi: 10.1021/acsearthspacechem.8b00093.

[156] S. K. Schum, B. Zhang, K. Dzepina, P. Fialho, C. Mazzoleni, and L. R. Mazzoleni, "Molecular and physical characteristics of aerosol at a remote free troposphere site: Implications for atmospheric aging," *Atmos Chem Phys*, vol. 18, no. 19, pp. 14017 – 14036, 2018, doi: 10.5194/acp-18-14017-2018.

[157] K. Gorkowski, T. C. Preston, and A. Zuend, "Relative-humidity-dependent organic aerosol thermodynamics via an efficient reduced-complexity model," *Atmos Chem Phys*, vol. 19, no. 21, pp. 13383–13407, 2019, doi: 10.5194/acp-19-13383-2019.

[158] F. Mahrt, E. Newman, Y. Huang, M. Ammann, and A. K. Bertram, "Phase Behavior of Hydrocarbon-like Primary Organic Aerosol and Secondary Organic Aerosol Proxies Based on Their Elemental Oxygen-to-Carbon Ratio," *Environ Sci Technol*, vol. 55, no. 18, pp. 12202–12214, doi: 10.1021/acs.est.1c02697.

[159] A. Maiboom, X. Tauzia, and J.-F. Hétet, "Experimental study of various effects of exhaust gas recirculation (EGR) on combustion and emissions of an automotive direct injection diesel engine," *Energy*, vol. 33, no. 1, pp. 22–34, 2008, doi: 10.1016/j.energy.2007.08.010.

[160] A. Tsolakis, A. Megaritis, M. L. Wyszynski, and K. Theinnoi, "Engine performance and emissions of a diesel engine operating on diesel-RME (rapeseed methyl ester) blends with EGR (exhaust gas recirculation)," *Energy*, vol. 32, no. 11, pp. 2072–2080, 2007, doi: 10.1016/j.energy.2007.05.016.

[161] M. Zheng, G. T. Reader, and J. G. Hawley, "Diesel engine exhaust gas recirculation—a review on advanced and novel concepts," *Energy Convers Manag*, vol. 45, no. 6, pp. 883–900, 2004, doi: 10.1016/S0196-8904(03)00194-8.

[162] J. B. Heywood, *Internal Combustion Engine Fundamentals*, 2nd ed. McGraw Hill Education, 2018.

[163] T. Li and H. Ogawa, "Analysis of the Trade-off between Soot and Nitrogen Oxides in Diesel-Like Combustion by Chemical Kinetic Calculation," *SAE Int J Engines*, vol. 5, no. 2, pp. 2011-01–1847, 2011, doi: 10.4271/2011-01-1847.

[164] K. Akihama, Y. Takatori, K. Inagaki, S. Sasaki, and A. M. Dean, "Mechanism of the Smokeless Rich Diesel Combustion by Reducing Temperature," *SAE Tech Pap*, 2001. doi: 10.4271/2001-01-0655.

[165] F. Bedford, C. Rutland, P. Dittrich, A. Raab, and F. Wirbeleit, "Effects of Direct Water Injection on DI Diesel Engine Combustion," *SAE Tech Pap*, 2000. doi: 10.4271/2000-01-2938.

[166] U. Asad and M. Zheng, "Efficacy of EGR and Boost in Single-Injection Enabled Low Temperature Combustion," *SAE Int J Engines*, vol. 2, no. 1, pp. 2009-01–1126, 2009, doi: 10.4271/2009-01-1126.

[167] V. Manente, B. Johansson, P. Tunestal, and W. J. Cannella, "Influence of Inlet Pressure, EGR, Combustion Phasing, Speed and Pilot Ratio on High Load Gasoline Partially Premixed Combustion," *SAE Tech Pap*, 2010. doi: 10.4271/2010-01-1471.

[168] C. Li, "Stratification and Combustion in the Transition from HCCI to PPC," Lund University, 2018. [Online]. Available: https:// lup.lub.lu.se/record/54165f85-8a5c-4050-88ec-6c1c577bd9e3.

[169] L. Hildingsson, G. Kalghatgi, N. Tait, B. Johansson, and A. Harrison, "Fuel Octane Effects in the Partially Premixed Combustion Regime in Compression Ignition Engines," *SAE Tech Pap*, 2009. doi: 10.4271/2009-01-2648.

[170] C. A. J. Leermakers, C. C. M. Luijten, L. M. T. Somers, G. T. Kalghatgi, and B. A. Albrecht, "Experimental Study of Fuel Composition Impact on PCCI Combustion in a Heavy-Duty Diesel Engine," *SAE Tech Pap*, 2011. doi: 10.4271/2011-01-1351.

[171] P. C. Bakker, J. E. de Abreu Goes, L. M. T. Somers, and B. H. Johansson, "Characterization of Low Load PPC Operation using RON70 Fuels," *SAE Tech Pap*, 2014. doi: 10.4271/2014-01-1304.

[172] İ. A. Reşitoğlu, K. Altinişik, and A. Keskin, "The pollutant emissions from diesel-engine vehicles and exhaust aftertreatment systems," *Clean Technol Environ Policy*, vol. 17, no. 1, pp. 15–27, 2015, doi: 10.1007/s10098-014-0793-9.

[173] Neha, R. Prasad, and S. V. Singh, "A review on catalytic oxidation of soot emitted from diesel fuelled engines," *J Environ Chem Eng*, vol. 8, no. 4, p. 103945, 2020, doi: 10.1016/j.jece.2020.103945.

[174] P. Ni, X. Wang, and H. Li, "A review on regulations, current status, effects and reduction strategies of emissions for marine diesel engines," *Fuel*, vol. 279, p. 118477, 2020, doi: 10.1016/j.fuel.2020.118477.

[175] R. L. vander Wal and A. J. Tomasek, "Soot oxidation: dependence upon initial nanostructure," *Combust Flame*, vol. 134, no. 1, pp. 1–9, 2003, doi: 10.1016/S0010-2180(03)00084-1.

[176] A. L. Boehman, J. Song, and M. Alam, "Impact of Biodiesel Blending on Diesel Soot and the Regeneration of Particulate Filters," *Energ Fuel*, vol. 19, no. 5, pp. 1857–1864, 2005, doi: 10.1021/ef0500585.

[177] B. Giechaskiel *et al.*, "Measurement of Automotive Nonvolatile Particle Number Emissions within the European Legislative Framework: A Review," *Aerosol Sci Technol*, vol. 46, no. 7, pp. 719–749, 2012, doi: 10.1080/02786826.2012.661103.

[178] L. Gren *et al.*, "Underground emissions and miners' personal exposure to diesel and renewable diesel exhaust in a Swedish iron ore mine," *Int Arch Occup Environ Health*, vol. 95, no. 6, pp. 1369–1388, 2022, doi: 10.1007/s00420-022-01843-x.

[179] Z. G. Liu, W. A. Eckerle, and N. A. Ottinger, "Gas-phase and semivolatile organic emissions from a modern nonroad diesel engine equipped with advanced aftertreatment," *J Air Waste Manage Assoc*, vol. 68, no. 12, pp. 1333–1345, 2018, doi: 10.1080/10962247.2018.1505676.

[180] S. Zeraati-Rezaei, M. S. Alam, H. Xu, D. C. Beddows, and R. M. Harrison, "Size-resolved physico-chemical characterization of diesel exhaust particles and efficiency of exhaust aftertreatment," *Atmos Environ*, vol. 222, p. 117021, 2020, doi: 10.1016/j.atmosenv.2019.117021.

[181] B. Giechaskiel, L. Ntziachristos, Z. Samaras, R. Casati, V. Scheer, and R. Vogt, "Effect of Speed and Speed-Transition on the Formation of Nucleation Mode Particles from a Light Duty Diesel Vehicle," *SAE Tech Pap*, 2007. doi: 10.4271/2007-01-1110.

[182] R. Suarez-Bertoa *et al.*, "On-road measurement of NH$_3$ emissions from gasoline and diesel passenger cars during real world driving conditions," *Atmos Environ*, vol. 166, pp. 488–497, 2017, doi: 10.1016/j.atmosenv.2017.07.056.

[183] T. Selleri, A. D. Melas, A. Joshi, D. Manara, A. Perujo, and R. Suarez-Bertoa, "An Overview of Lean Exhaust deNOx Aftertreatment Technologies and NOx Emission Regulations in the European Union," *Catalysts*, vol. 11, no. 3, 2021, doi: 10.3390/catal11030404.

[184] A. bin Aziz, "High Octane Number Fuels in Advanced Combustion Modes for Sustainable Transportation," Lund University, 2020. [Online]. Available: https://lup.lub.lu.se/record/36d51b09-d87b-43d5-b7a2-5abf30495ac6

[185] P. Tunestål, "TDC Offset Estimation from Motored Cylinder Pressure Data based on Heat Release Shaping," *Oil & Gas Science and Technology – Revue d'IFP Energies nouvelles*, vol. 66, no. 4, pp. 705–716, 2011, doi: 10.2516/ogst/2011144.

[186] B. Johansson, Ö. Andersson, P. Tunestål, and M. Tunér, *Combustion Engines*, vol. 1. Lund University, 2014.

[187] H. Solaka, M. Tuner, B. Johansson, and W. Cannella, "Gasoline Surrogate Fuels for Partially Premixed Combustion, of Toluene Ethanol Reference Fuels," *SAE Tech Pap*, 2013. doi: 10.4271/2013-01-2540.

[188] K. Kar and W. K. Cheng, "Speciated Engine-Out Organic Gas Emissions from a PFI-SI Engine Operating on Ethanol/Gasoline Mixtures," *SAE Int J Fuels Lubr*, vol. 2, no. 2, 2009, doi: 10.4271/2009-01-2673.

[189] T. Wallner, "Correlation Between Speciated Hydrocarbon Emissions and Flame Ionization Detector Response for Gasoline/Alcohol Blends," *J Eng Gas Turbine Power*, vol. 133, no. 8, 2011, doi: 10.1115/1.4002893.

[190] W. Schindler, C. Haisch, H. A. Beck, R. Niessner, E. Jacob, and D. Rothe, "A Photoacoustic Sensor System for Time Resolved Quantification of Diesel Soot Emissions," *SAE Tech Pap*, 2004. doi: 10.4271/2004-01-0968.

[191] Cambustion Limited, "Fast Response Aerosol Size Measurements with the DMS500." www.cambustion.com/products/dms500/aerosol (accessed Sep. 05, 2022).

[192] M. R. Canagaratna *et al.*, "Chemical and microphysical characterization of ambient aerosols with the aerodyne aerosol mass spectrometer," *Mass Spectrom Rev*, vol. 26, no. 2, pp. 185–222, 2007, doi: 10.1002/mas.20115.

[193] T. B. Onasch *et al.*, "Soot Particle Aerosol Mass Spectrometer: Development, Validation, and Initial Application," *Aerosol Sci Technol*, vol. 46, no. 7, pp. 804–817, 2012, doi: 10.1080/02786826.2012.663948.

[194] E. Kang, M. J. Root, D. W. Toohey, and W. H. Brune, "Introducing the concept of Potential Aerosol Mass (PAM)," *Atmos Chem Phys*, vol. 7, no. 22, pp. 5727–5744, 2007, doi: 10.5194/acp-7-5727-2007.

[195] E. Mancaruso, B. Vaglieco, and C. Ciaravino, "Combustion Analysis in an Optical Diesel Engine Operating with Low Compression Ratio and Biodiesel Fuels," *SAE Tech Pap*, 2010. doi: 10.4271/2010-01-0865.

[196] S. K. Hoekman and C. Robbins, "Review of the effects of biodiesel on NOx emissions," *Fuel Process Technol*, vol. 96, pp. 237–249, 2012, doi: 10.1016/j.fuproc.2011.12.036.

[197] U. Horn, R. Egnell, B. Johansson, and Ö. Andersson, "Detailed Heat Release Analyses with Regard to Combustion of RME and Oxygenated Fuels in an HSDI Diesel Engine," *SAE Tech Pap*, 2007. doi: 10.4271/2007-01-0627.

[198] M. S. Graboski and R. L. McCormick, "Combustion of fat and vegetable oil derived fuels in diesel engines," *Prog Energy Combust Sci*, vol. 24, no. 2, pp. 125–164, 1998, doi: 10.1016/S0360-1285(97)00034-8.

[199] M. Pawlyta, J.-N. Rouzaud, and S. Duber, "Raman microspectroscopy characterization of carbon blacks: Spectral analysis and structural information," *Carbon N Y*, vol. 84, pp. 479–490, 2015, doi: 10.1016/j.carbon.2014.12.030.

[200] P. Tornehed and U. Olofsson, "Modelling lubrication oil particle emissions from heavy-duty diesel engines," *Int J Engine Res*, vol. 14, no. 2, pp. 180–190, 2013, doi: 10.1177/1468087412452208.

[201] D. R. Gentner *et al.*, "Review of Urban Secondary Organic Aerosol Formation from Gasoline and Diesel Motor Vehicle Emissions," *Environ Sci Technol*, vol. 51, no. 3, pp. 1074–1093, Feb. 2017, doi: 10.1021/acs.est.6b04509.

[202] G. Lequien, Ö. Andersson, P. Tunestal, and M. Lewander, "A Correlation Analysis of the Roles of Soot Formation and Oxidation in a Heavy-Duty Diesel Engine," *SAE Tech Pap*, 2013. doi: 10.4271/2013-01-2535.

[203] S. Shamun *et al.*, "Exhaust PM Emissions Analysis of Alcohol Fueled Heavy-Duty Engine Utilizing PPC," *SAE Int J Engines*, vol. 9, no. 4, pp. 2142–2152, 2016, doi: 10.4271/2016-01-2288.

[204] P. Kheirkhah, P. Kirchen, and S. Rogak, "Measurement of cycle-resolved engine-out soot concentration from a diesel-pilot assisted natural gas direct-injection compression-ignition engine," *Int J Engine Res*, vol. 23, no. 3, pp. 380–396, 2022, doi: 10.1177/1468087420986263.

[205] J. Yon, A. Bescond, and F. Liu, "On the radiative properties of soot aggregates part 1: Necking and overlapping," *J Quant Spectrosc Radiat Transf*, vol. 162, pp. 197–206, 2015, doi: https://doi.org/10.1016/j.jqsrt.2015.03.027.

[206] A. G. Sappok and V. W. Wong, "Detailed Chemical and Physical Characterization of Ash Species in Diesel Exhaust Entering Aftertreatment Systems," *SAE Tech Pap*, 2007. doi: 10.4271/2007-01-0318.

[207] H. Wang, "Formation of nascent soot and other condensed-phase materials in flames," *Proc Combust Inst*, vol. 33, no. 1, pp. 41–67, 2011, doi: 10.1016/j.proci.2010.09.009.

[208] M. Crippa *et al.*, "Wintertime aerosol chemical composition and source apportionment of the organic fraction in the metropolitan area of Paris," *Atmos Chem Phys*, vol. 13, no. 2, pp. 961–981, 2013, doi: 10.5194/acp-13-961-2013.

[209] J. L. Jimenez *et al.*, "Evolution of Organic Aerosols in the Atmosphere," *Science (1979)*, vol. 326, no. 5959, pp. 1525–1529, 2009, doi: 10.1126/science.1180353.

[210] M. D. Petters and S. M. Kreidenweis, "A single parameter representation of hygroscopic growth and cloud condensation nucleus activity," *Atmos Chem Phys*, vol. 7, no. 8, pp. 1961–1971, 2007, doi: 10.5194/acp-7-1961-2007.

[211] H. Tost and K. J. Pringle, "Improvements of organic aerosol representations and their effects in large-scale atmospheric models," *Atmos Chem Phys*, vol. 12, no. 18, pp. 8687–8709, 2012, doi: 10.5194/acp-12-8687-2012.

[212] P. Hlaing, A. Said, E. Cenker, H. G. Im, and J. Turner, "Comparing Unburned Fuel Emission from a Pre-chamber Engine Operating on Alcohol Fuels using FID and FTIR Analyzers," *SAE Tech Pap*, 2022. doi: 10.4271/2022-01-1094.

[213] D. Posnett, "Decarbonisation today dramatically reduces future challenges," *EURACTIV*, 2022. Accessed: Oct. 24, 2022. [Online]. Available: https://www.euractiv.com/section/biofuels/opinion/decarbonisation-today-dramatically-reduces-future-challenges/

About the author

Maja Novaković, an engineer, a friend, a daughter, a wife, and a mother, obtained her BSc degree at the University of Belgrade in Serbia, followed by an MSc degree at Karlstad University, Sweden. Both in the field of Electrical Engineering with specialization in Signals and Systems.

A winner of the environmental grant from The Swedish Association of Graduate Engineers, she has been using her problem-solving skills to discover ways to cut air pollution and fight climate change within a research project at the Department of Energy Sciences at Lund University in Sweden. This doctoral thesis is a compilation of her research results.

LUND
UNIVERSITY